Available online at www.sciencedirect.com
SCIENCE DIRECT®
Journal of Theoretical Biology 238 (2006) 616–635
Journal of Theoretical Biology
www.elsevier.com/locate/yjtbi

Uncovering the design principles of circadian clocks: Mathematical analysis of flexibility and evolutionary goals

D.A. Rand[a,*], B.V. Shulgin[a], J.D. Salazar[a,b], A.J. Millar[b,1]

[a]Interdisciplinary Programme in Cellular Regulation & Mathematics Institute, University of Warwick, Coventry CV4 7AL, UK
[b]Interdisciplinary Programme in Cellular Regulation & Department of Biological Sciences, University of Warwick, Coventry CV4 7AL, UK

Received 29 September 2004; received in revised form 11 April 2005; accepted 15 June 2005
Available online 18 August 2005

Abstract

In this paper, we present the mathematical details underlying both an approach to the flexibility of regulatory networks and an analytical characterization of evolutionary goals of circadian clock networks. A fundamental problem in cellular regulation is to understand the relation between the form of regulatory networks and their function. Circadian clocks present a particularly interesting instance of this. Recent work has shown that they have complex structures involving multiple interconnected feedback loops with both positive and negative feedback. We address the question of why they have such a complex structure and argue that it is to provide the flexibility necessary to simultaneously attain multiple key properties of circadian clocks such as robust entrainment and temperature compensation. To do this we address two fundamental problems: (A) to understand the relationships between the key evolutionary aims of the clock and (B) to ascertain how flexible the clock's structure is. To address the first problem we use infinitesimal response curves (IRCs), a tool that we believe will be of general utility in the analysis of regulatory networks. To understand the second problem we introduce the flexibility dimension d, show how to calculate it and then use it to analyse a range of models. We believe our results will generalize to a broad range of regulatory networks.

Keywords: Circadian clocks; Gene expression; Feedback loops; Oscillations; Mathematical models; Flexibility

1. Introduction

Current descriptions of the molecular circadian clock have a negative feedback loop with delay at their heart (Young and Kay, 2001; Johnson et al., 2003; Roenneberg and Merrow, 2003). Indeed, a single such feedback loop with a very simple structure will produce robust oscillations (Goldbeter, 2002a,b). It is therefore pertinent to ask why current understanding of the regulatory networks of these clocks suggests that they almost universally have a much more complicated structure with multiple interlocking feedback loops with both negative and positive feedback. Several authors have written about the reasons for this complexity (Johnson et al., 2003; Roenneberg and Merrow, 2003; Smolen et al., 2001; Cheng et al., 2001; Cyran et al., 2003; Glossop et al., 1999; Lee et al., 2000; Ueda et al., 2001; Preitner et al., 2002; Reddy et al., 2002; Daan et al., 2001; Albrecht et al., 2001). The primary reason (though not the only one) suggested is robustness either to parameter perturbations or to stochastic noise. However, it has not been shown that the observed structure leads to robustness and there is no convincing explanation of why one would expect this. Of course, it is likely that some of the complexity arises from specific needs of the organism in question. Nevertheless, it is important to consider whether there are general principles behind the form of the structures observed. That importance is reinforced by the fact that the disparate clock mechanisms maintain biological rhythms in a very similar

*Corresponding author. Tel.: +44 24 7652 3599; fax: +44 24 7652 4182.
E-mail address: dar@maths.warwick.ac.uk (D.A. Rand).
[1]Present address: Institute of Molecular Plant Sciences, University of Edinburgh, Mayfield Road, Edinburgh EH9 3JH, UK.

0022-5193/$ - see front matter © 2005 Elsevier Ltd. All rights reserved.
doi:10.1016/j.jtbi.2005.06.026

fashion in all organisms and seem to be a product of convergent evolution (Young and Kay, 2001). In this paper, we address this question by considering differential equation models of the clock. We show that clocks involving a single loop are inflexible in a precise sense and that the degree of flexibility of a clock network is related to the complexity of the loop structure. Then we present an analysis of why this flexibility is important for the functioning of the clock.

Circadian oscillators are entrained by the daily cycles of light and temperature (Johnson et al., 2003). Entrainment by light is generally considered to work by modulating a small number of particular parameters of the regulatory network such as certain degradation or expression rates. For temperature the mechanism is less clear. It is generally assumed that temperature fluctuations affect many more rates and it is unclear how these combine (Rensing and Ruoff, 2002). For entrainment by light or temperature to work it is therefore important that a clock is sensitive to fluctuations in either of these environmental factors. On the other hand, an important property of many clocks is that key characteristics such as period are not sensitive to sustained changes in, for example, temperature (Johnson et al., 2003). To analyse the relations between these possibly conflicting goals we introduce a tool, *infinitesimal response curves*, which allows us to characterise the stability and entrainment properties of the clock.

The phenotype of the clock is largely determined by the set of characteristics describing, for example, how it is entrained by light and temperature, the phase relationships between the protein products, the coordination of output pathways, which phases (e.g. dawn and dusk) it can track, its response to both sustained and stochastic changes in environmental variables such as temperature and pH and its robustness to internal fluctuations of the molecular environment of the cell. These characteristics are largely set by the network structure of the clock and the values of the various parameters (such as rate constants) describing the quantitative structure of the interactions. Thus we can regard evolution as acting on both the network structure and the parameters by small changes, as revealed by the natural genetic variation (Johnson et al., 2003) in *Arabidopsis*, *Drosophila* and the mouse. Though larger changes occur such as deletion of core genes, they do not seem to be maintained and thus we do not consider them here.

Evolution will seek to simultaneously tune the multiple and possibly conflicting characteristics of the sort described above. To understand how this can be achieved one first has to address two problems:

(A) one must understand the relationships between the various characteristics (e.g. to what extent they can be tuned independently and which of them are strongly related);

(B) one must ascertain how flexible the clocks structure is, i.e., how easy it is to simultaneously tune for the multiple goals.

Table 1
A list of the models considered together with the number of state variables n and the number of parameters s

Model	n	s
Leloup et al. (1999) *Neurospora*	3	10
Leloup et al. (1999) *Drosophila*	10	38
Ueda et al. (2001) *Drosophila*	10	55
Leloup and Goldbeter (2003) mammal	16	53
Forger and Peskin (2003) mammal	73	36

The ratio of s to n is anomalously small for the Forger–Peskin model (Forger and Peskin, 2003) because in it several groups of parameters are assigned the same values and are regarded as the same parameter.

To address the first problem, A, we show that the key goals can be expressed in terms of certain system variables so that each goal corresponds to tuning one or more of these variables to certain prescribed values. Our analysis will show that there is a significant number of effectively independent quantities that evolution has to tune and one is able to determine which combinations of parameters should be tuned in order to move towards the realization of a specific circadian characteristic.

For problem B we introduce a measure of the flexibility, called the *flexibility dimension* d, that is an important quantity because it tells us how many key output variables evolution is able to tune at any time and in how many dimensions evolution can move the system. We produce evidence that this flexibility is much lower than one might expect from the fact that all clock systems depend upon a relatively large number s of parameters such as rate or coupling constants. For the published models considered in Table 1, s ranges from 9 to over 50 and in reality the number of parameters is likely to be higher. On the face of it the large number of tuneable parameters suggests that there is a huge flexibility to explore and optimize key characteristics of the clock. However, our analysis shows that d is much smaller than s, usually by an order of magnitude and is roughly proportional to the *loop complexity* of the network as described below.

It follows from the definition of the flexibility dimension d that if there are q key independent evolutionary target variables or characteristics, the realization of these will be effectively impossible if d is smaller than q. Thus there is a selective advantage in increasing d to a value where the full range of key evolutionary targets can be tuned. Since, our analysis of problem A will indicate that the number q of essentially independent evolutionary targets is relatively large, it follows that for simple networks there is selective pressure for increased loop complexity.

These results suggest that, faced with the need to address multiple independent goals, evolution will have used a strategy of decorating the minimal regulatory module with extra structure in order to obtain the necessary flexibility.

2. Key clock characteristics

The literature now contains a broad range of explicitly molecular models for circadian clocks that are mathematically defined by differential equations (Goldbeter, 2002a,b; Tyson et al., 1999, see Table 1). Differential equations provide the most appropriate framework in which to address the questions we are concerned with here because the analytical tools such as IRCs and the theoretical ideas around flexibility are most readily developed in this context. Our analysis is not specific to any of these models but in Table 1 we list a number of them that will be used to illustrate the points we make. All these models display sustained oscillations in the appropriate parameter regimes and are entrained by light–dark cycles of appropriate intensity. This sustained oscillation is described by a (stable) limit cycle.

There is a relatively large number of key characteristics of clocks. In this section we discuss some important examples. In later sections we will show how to describe these characteristics in terms of infinitesimal response curves.

Clearly clocks must be robustly entrained by commonly occurring environmental signals. The phase of entrainment must be appropriate. These aspects must persist with the different environmental conditions arising during the course of a year. They should be stable to commonly encountered environmental variations such as those of temperature, pH, nutrition or growth conditions. Because there is only a finite number of molecules involved, perhaps even a relatively small number, the clocks are intrinsically stochastic. Therefore, the clock should be adjusted so that the period and phase relationships are relatively robust to these stochastic fluctuations and the clock should function reliably in the presence of internal noise due to the fluctuation in the molecular environment of the cell. It has been suggested that, depending on the organism, the clock is regulating the expression of several hundred to more than a thousand genes (Harmer et al., 2000). It is therefore important that appropriate phase relationships for the protein products driving output pathways are maintained. These phase relationships should also be robust to the sort of perturbations discussed above.

2.1. Robust entrainment by environmental signals

The most basic requirement for a clock is that the relevant 24 h environmental cycles should entrain it in a robust way. Moreover, this entrainment needs to be maintained in the face of perturbations such as environmental and stochastic fluctuations.

To clarify the issues associated with robust entrainment it may help to consider an approximate model of the clock which is valid when the limit cycle γ_0 of the clock in darkness (i.e. with no forcing) attracts nearby orbits sufficiently quickly (Fig. 1). If this is the case, in light–dark (L–D) cycles with a long enough dark period, the state of the clock at the end of the dark period will be close to a state on γ_0. Thus the Poincaré map of the clock in L–D cycles maps a small neighbourhood of γ_0 into another small neighbourhood of γ_0. If we therefore mark each point on γ_0 by its phase ϕ ($0 \leqslant \phi \leqslant \tau$ where τ is the period), the Poincaré map is approximated by the map $\phi_n \to \phi_{n+1} = F(\phi_n)$, where ϕ_n is the phase at dawn on the nth day and ϕ_{n+1} is the phase at dawn on day $n+1$. See Figs. 1 and 2 for a schematic representation of this construction and an example of what the mapping F will look like. It is natural to consider the function $\Phi(\phi) = F(\phi) - \phi - (L - \tau)$ where $L - \tau$ is the *circadian correction*, i.e. the difference between the length of the day L and the period τ of the oscillator in continuous darkness. Then Φ can be regarded as a phase response curve and F has the following form:

$$\phi_{n+1} = F(\phi_n) = \phi_n + \Phi(\phi_n) + (L - \tau). \tag{1}$$

Another way of looking at this equation is as follows: consider a situation where light has a given intensity and acts from dawn for S hours. Let $\Phi(\phi)$ be the phase change associated with applying this light when dawn coincides with the phase ϕ. If the phase at dawn is ϕ_n then at dusk it is $\phi_n + S + \Phi(\phi_n)$. Therefore at the end of the day the phase is given by Eq. (1).

The mapping F has a fixed point ($F(\phi_*) = \phi_*$) at ϕ_* provided $\Phi(\phi_*) = \tau - L$. The local stability of this fixed point ϕ_* is determined by the slope of F at ϕ_*. If $\chi = |F'(\phi_*)| < 1$ then ϕ_* is (locally) stable ($\phi_n = F^n(\phi_0) \to \phi_*$ as $n \to \infty$ for all ϕ near ϕ_*, where $F^n = F \circ \cdots \circ F$ (n times)). Therefore this fixed point is stable provided $-2 < \Phi'(\phi_*) < 0$. Entrainment corresponds to the existence of such a stable fixed point ϕ_* and ϕ_* tells us the phase of the entrained state.

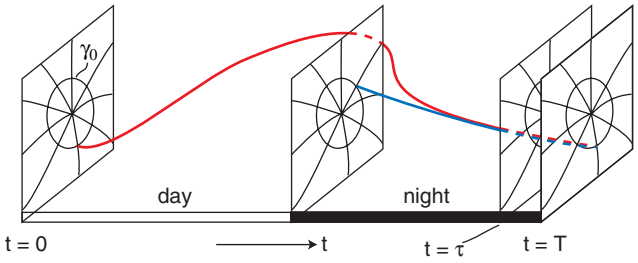

Fig. 1. A schematic representation of the discussion justifying the approximation used to derive Eq. (1).

If we change parameters we can expect that both the shape of the graph of F as reflected in Φ and the circadian correction $L-\tau$ will change. This will in turn shift the point ϕ_* and may even cause the graph of F to move above or below the diagonal $\phi_{n+1}=\phi_n$ so that there is no such fixed point and the system looses its entrainment.

Consider, for example, changes caused by a change in temperature. Temperature T will presumably affect a number of parameters k_i which will be functions of T. It follows that while the stable fixed point exists, its position and its stability exponent χ depend upon T: $\phi_*=\phi_*(T)$ and $\chi=\chi(T)$. What is required is that $\phi_*=\phi_*(T)$ and $\chi(T)$ are roughly independent of temperature T. This ensures that the entrainment persists and remains stable in different temperature regimes. If the shape of Φ does not vary much with parameter changes then we see from Eq. (1) and Fig. 2 that the crucial thing is that the period τ does not change too much with temperature. It is this that has been observed experimentally (Rensing and Ruoff, 2002). This stability of the period under temperature changes is referred to as *temperature compensation*. We will consider these aspects further in Section 5.2 when we have introduced the tools we need for a characterization.

This need for robustness of the phase of entrainment and its stability would seem to apply under more general situations; for example, in the face of general parameter perturbations and intrinsic and extrinsic stochasticity.

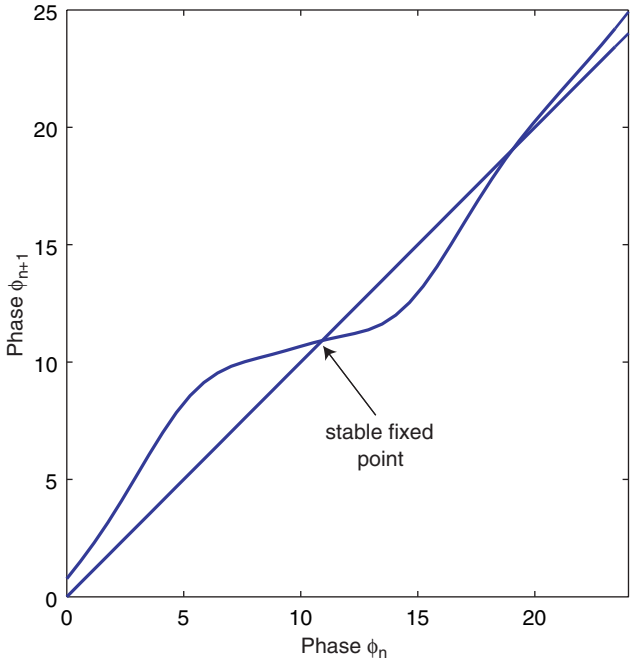

Fig. 2. Representation of the mapping F given by Eq. (1).

3. Flexibility and evolutionary accessibility

All clock systems depend upon a relatively large number s of parameters. These parameters, for example, determine the functional descriptions of transcription, translation, (de)phosphorylation, degradation and binding. They include all the rate constants and all the maximum rates of transcription, translation and protein modification. We denote these parameters by k_i and collect then into a vector $k=(k_1,\ldots,k_s)$. For the published models considered in Table 1, s ranges from 9 to over 50 and in reality the number of parameters is likely to be higher.

Varying the parameters $k=(k_1,\ldots,k_s)$ causes output characteristics $Q_j=Q_j(k)$ to change. The outputs Q_j we consider will include quantities such as period, the phases of the maxima and minima of mRNA and proteins, the amplitude of these maxima and minima, and the levels of mRNA and protein at prescribed phases. They can also be functions rather than numbers; for instance a phase response curve. All of the outputs Q_j we consider are functions of the limit cycle, i.e. you only need to know the limit cycle to know the value of the output Q_j. Usually we consider several outputs Q_j simultaneously and then we collect then into a vector $Q=(Q_j)$. For example, we may wish to simultaneously tune these several outputs.

When the parameters are changed (usually by small amounts) then the variation is denoted by $\delta k=(\delta k_1,\ldots,\delta k_s)$ (so that the new parameter values are given by $k+\delta k$), and the change caused in an output such as Q_j is denoted by δQ_j.

Each variation of the parameters from $k_1,\ldots,k_s$ to $k_1+\delta k_1,\ldots,k_s+\delta k_s$ will cause the limit cycle to vary and this in turn changes the vector of output characteristics $Q=(Q_j)$ by an amount $\delta Q=(\delta Q_j)$.

The variation $\delta k=(\delta k_i)$ is an absolute one in that the size of the changes δk_i bears no relation to the size of the parameter values k_i that we are varying about. For the models we consider the k_is can vary over more than one order of magnitude. It is therefore often more appropriate to consider the proportional variation in a parameter which is given by $\delta\eta_i=\delta k_i/k_i$. These changes also have the important advantage of being dimensionless. We say that such variations are *proportional*.

We could also do a similar scaling for the output variations δQ_j. However, we do not do this because (a) we assume that the output variables have been chosen so that they are dimensionless and so that their sizes are all of the same order of magnitude, and (b) because later we will consider the case where δQ is the actual variation in the limit cycle, in which case such a scaling is not natural. One can usually ensure that (a) is true by dividing the quantity Q_i by an appropriate scale. For example, rather than consider period p as one of the output variables, take p/L where L is daylength.

If the variations δk_i are small then the relationship between δk and δQ is approximately linear and given by a matrix $M = (M_{ij})$ where $\delta Q_j = \sum_i M_{ij}\delta k_i$ is the change to Q_j caused by a change in k of δk. The numbers M_{ij} are sometimes called the *linear sensitivities* of the quantity Q_j (Hwang et al., 1978).

Thus $\delta Q = M \cdot \delta k$. In terms of the scaled parameter changes $\delta\eta$, the change δQ in Q is given by

$$\delta Q = M \cdot \Delta_k \cdot \delta\eta, \tag{2}$$

where Δ_k is the diagonal matrix $\mathrm{diag}(k_1, \ldots, k_s)$.

The large number of tuneable parameters would seems to suggest that there is a huge flexibility to simultaneously explore and optimize key characteristics of the clock such as those discussed above. However, even when the parameter variations can freely explore all the parameter combinations, the direction of the resultant changes in a given vector $Q = (Q_j)$ of outputs may be highly non-uniform, with the result that many output changes are capable of being reached only with great difficulty or not at all. A good picture to have in mind is of a round s-dimensional ball B of parameter variations with small radius ε centred on the base parameter value k. If ε is sufficiently small, the image E of B will be approximately an ellipsoid and the size of its axes $\sigma_1 > \sigma_2 > \ldots$ of this ellipsoid (ordered by magnitude) may well decrease very rapidly. In this case most random variations in the parameters will produce output changes δQ that are lined up with the axes with the largest size σ_i. Then if e is a unit vector in such a direction and the N random parameter variations produce output changes $\delta Q^{(\ell)}$, $\ell = 1, \ldots, N$, the correlation

$$\frac{\sum_\ell \langle \delta Q^{(\ell)}, e\rangle^2}{\|e\|^2 \sum_\ell \|\delta Q^{(\ell)}\|^2}$$

will be relatively large. In fact, it will be proportional to the square of the magnitude of the axis. Another way of looking at his is to say that output variations δQ in the directions corresponding to the other axes are inaccessible in the sense that they will require changes δk in the parameters for which the ratio of magnitudes $\|\delta Q\|/\|\delta k\|$ is very small. These two ways of looking at it are essentially equivalent as we show below.

The reader should note that these notions of accessibility given below are applied in the linear regime. The changes δQ and the parameter δk needed to achieve them are small even though in the inaccessible case the size of δk may be much greater than δQ. We are not considering the case where δQ is so large (and inaccessible) that δk must be so large that the perturbation is outside the region where the linear approximation is accurate.

3.1. The approach via targeted parameter variations

We fix a vector $Q = (Q_j)$ which represents a particular set of outputs and firstly define the flexibility dimension in terms of Q. For example, Q might be the vector whose entries are the phases of all the maxima and minima of all mRNA and protein products and all amplitudes of the oscillations in these products. Later, we will define the flexibility dimension which applies to the complete set of output variables determined by the limit cycle.

A proportional parameter change $\delta\eta$ gives rise to a change in the outputs of $\delta Q = M' \cdot \delta\eta$ where $M' = M \cdot \Delta_k$. For a given output δQ consider the set of all proportional parameter changes $\delta\eta$ such that $M' \cdot \delta\eta = \delta Q$. Let $R_{\delta Q}$ be the supremum of the ratios $\|\delta Q\|/\|\delta\eta\|$ for $\delta\eta$ in this set, i.e.

$$R_{\delta Q} = \sup\left\{\frac{\|\delta Q\|}{\|\delta\eta\|} : M' \cdot \delta\eta = \delta Q\right\}. \tag{3}$$

Since δQ and $\delta\eta$ are linearly related $R_{\delta Q}$ does not depend upon the size of δQ but only on its direction.

For accessibility we require that $R_{\delta Q}$ is not too small, because otherwise the given output change can only be obtained by an excessively large parameter change. However, usually we do not want to measure accessibility in absolute terms but in terms which relate it to the most accessible output. Thus we also consider

$$R^* = \sup_{\delta Q} R_{\delta Q}.$$

Therefore, we fix a small number ε and define the *accessible cone* $C(k, \varepsilon)$ to consist of all vectors δQ such that $R_{\delta Q}$ is greater than εR^*.

If Q is scaled (i.e. all the Q_i are scaled by the same amount) then $R_{\delta Q}$ and R^* are scaled in the same way and therefore there is no change in the accessible cone. However, if each of the Q_j are scaled by a different amount, there may be changes, but this is easy to calculate and take account of.

Definition 1. The *flexibility dimension* d of the output vector $Q = (Q_j)$ is the largest dimension of any linear subspace that is contained in the accessible cone $C(k, \varepsilon)$.

Roughly speaking, if W is such a subspace then all accessible vectors δQ are of the form $w + \zeta$ where w is in W and, compared to w, the magnitude of ζ is extremely small (of order ε). Thus, neglecting these relatively very small adjustments ζ, the set of accessible vectors is d-dimensional.

3.1.1. Singular values and the flexibility dimension

Consider a $m \times r$ matrix B whose number of rows m is greater than or equal to the number of columns r. Every such B can be written as

$$B = UDV^t, \tag{4}$$

where U is a $m \times r$ orthonormal matrix ($UU^t = I_m$ and $U^t U = I_r$), V is a $r \times r$ orthonormal matrix and $D = \mathrm{diag}(\sigma_1, \ldots, \sigma_r)$ is a diagonal matrix. This representation is called the Singular Value Decomposition (SVD) of B (Press et al., 1988). The elements $\sigma_1 \geqslant \cdots \geqslant \sigma_r$ are called the *singular values* of B. From (4) one immediately deduces that $B \cdot v_j = \sigma_j u_j$ where v_j and u_j are, respectively, the columns of V and U corresponding to the singular value σ_j. The columns v_j of V with $\sigma_j = 0$ provide an orthonormal basis for the kernel of B ($v_j \cdot v_k = \delta_{jk}$) and the columns u_j of U with $\sigma_j \neq 0$ are an orthonormal basis for the image or range of B.

Since the relationship between scaled parameters and outputs is given by $\delta Q = M \cdot \Delta_k \cdot \delta\eta$, we study the singular value decomposition of $M' = M \cdot \Delta_k$. For this matrix, r is the number of parameters s, and m is the number of outputs δQ_j considered.

Theorem 2. *The flexibility dimension d of the output vector $Q = (Q_j)$ is given by the number of singular values σ_j of M' with $\sigma_j/\sigma_1 > \varepsilon$.*

This result provides an effective and practical way of calculating the flexibility dimension as it is relatively easy to compute M and hence M'. The proof is given in Appendix A (Section A.1).

If one wants to measure flexibility in absolute terms where $R_{\delta Q}$ is compared to ε itself rather than εR^*, then the dimension is given by the number of singular values σ_j of M' with $\sigma_j > \varepsilon$. In fact, the numbers σ_j give the length of the axes of the ellipsoid E described above.

Note: In many cases of interest (and in all the examples in Table 1), the σ_j decrease very fast. This means that the dependence of the flexibility dimension on ε is relatively weak. For example, when the σ_j decrease at least exponentially then the growth in d as ε is decreased is at most proportional to $\log 1/\varepsilon$.

3.2. The approach via random variations of parameters

Alternatively, we can define the accessible cone by considering random variations where the output vectors $\delta Q^{(\ell)} = (\delta Q_j^{(\ell)})$, $(\ell = 1, 2, \ldots, N)$, arise from a large number N of variations $\delta k_i^{(\ell)} = k_i \delta\eta_i^{(\ell)}$ where the proportions $\delta\eta_i^{(\ell)}$ are zero-mean independent identically distributed random variables. We compare the variance of the projection of the $\delta Q^{(\ell)}$ onto a given vector δQ with the variance of the sizes $\|\delta Q^{(\ell)}\|$, i.e. we consider the ratio

$$(R'_{\delta Q})^2 = \lim_{N\to\infty} \frac{\sum_\ell \langle \delta Q^{(\ell)}, \delta Q\rangle^2}{\|\delta Q\|^2 \sum_\ell \|\delta Q^{(\ell)}\|^2}.$$

We then define the accessible cone by

$$C'(\varepsilon, k) = \{\delta Q : R'_{\delta Q} \geqslant \varepsilon\}. \tag{5}$$

3.2.1. Principal components: the optimal orthogonal basis for projecting the outputs $\delta Q^{(\ell)}$

Suppose for example, that one is considering a random set of perturbations and corresponding outputs $\delta Q^{(\ell)}$, $\ell = 1, \ldots, N$, as above. Consider any orthonormal basis $e = (e_j)$ of the space of output vectors δQ ($\|e_j\| = 1$ and $e_i \cdot e_j = 0$ if $i \neq j$). Let

$$err_k(\delta Q^{(\ell)}) = \left\| \delta Q^{(\ell)} - \sum_{j=1}^{k} (\delta Q^{(\ell)} \cdot e_j) e_j \right\|^2$$

denote the size of the error if we approximate $\delta Q^{(\ell)}$ by its projection onto the subspace spanned by the first k elements of the basis. Then

$$err_k(\delta Q^{(\ell)}) = \sum_{j=k+1}^{\infty} (\delta Q^{(\ell)} \cdot e_j)^2$$

because the basis is orthonormal. We seek to find the basis $e = (e_j)$ which for all $k \geqslant 1$ minimizes

$$v_k^2 = \frac{1}{N} \sum_\ell err_k(\delta Q^{(\ell)}) = \frac{1}{N} \sum_\ell \sum_{j=k+1}^{\infty} (\delta Q^{(\ell)} \cdot e_j)^2,$$

the average of err_k over all outputs $\delta Q^{(\ell)}$. Since the mean of the δQ^{ℓ} is zero, v_k^2 is the variance of the error projected onto the directions e_j with $j > k$.

The basis minimising the v_k^2 for all $k \geqslant 1$ is given by the eigenvectors e_j of the self-adjoint linear operator $\mathbf{Y}$ defined by $\mathbf{Y} \cdot e = N^{-1} \sum_\ell (\delta Q^{(\ell)} \cdot e) e$ (ordered by decreasing size of their corresponding eigenvalue) and for this basis the corresponding eigenvalue is v_i^2. A matrix representation of this operator is given by taking the matrix A whose columns are the vectors $\delta Q^{(i)}$ and forming the matrix $\mathbf{Y} = N^{-1} A A^t$. This is a matrix of size (dim δQ) $\times$ (dim δQ). Because it is self-adjoint ($\mathbf{Y}^t = \mathbf{Y}$), its eigenvalues are always real and its eigenvectors form an orthogonal basis. The pairs (e_j, v_j) consisting of the vector e_j and corresponding eigenvalue $v_j \geqslant 0$ are called the *principal components* of the ensemble $\{\delta Q^{(\ell)}\}$.

If we write $\delta Q^{(\ell)} = \sum_j a_j^{(\ell)} e_j$ as above then the $\delta Q^{(\ell)}$ are mainly in the direction of the principal components e_j with the largest v_j. Moreover, if $v_k \leqslant \varepsilon$ then the ratio of the variance of the lengths of the vectors $\delta Q^{(\ell)} - \sum_{j=1}^{k} a_j^{(\ell)} e_j$ to the variance of the lengths of the vectors $\delta Q^{(\ell)}$ is of order ε^2, $O(\varepsilon^2)$.

The following theorem relates the principal components, the SVD of M' and the cone $C'(\varepsilon, k)$.

Theorem 3. *If the components $\delta\eta_i^{(\ell)}$ of the vector $\delta\eta^{(\ell)}$ are independent then, in the limit $N \to \infty$, the maximal dimension d' of a linear subspace in the cone $C'(\varepsilon, k)$ is the number of singular values σ_j of M' with $\sigma_j^2 > \varepsilon^2 \Xi$ where $\Xi = \sum_j \sigma_j^2$.*

As above, $M' = UDV^t$ is the singular value decomposition of M', u_j denotes the jth column of U,

$m = \dim \delta Q$ and $D = \mathrm{diag}(\sigma_1, \ldots, \sigma_m)$ is the matrix of singular values.

Thus we see that the cones $C(\varepsilon_1, k)$ and $C'(\varepsilon_2, k)$ are equal if

$$\varepsilon_1 = \varepsilon_2 \sqrt{1 + \sum_{j \geqslant 2} (\sigma_j/\sigma_1)^2}.$$

Since, typically the singular values decrease quickly the square root term is no too far from one. For the examples in Table 2 it takes the following approximate values: 1.01, 1.2, 1.003, 1.02 and 1.38. In this sense both approaches give the same flexibility dimension.

3.2.2. Definition of the clock's flexibility dimension

As defined above the flexibility dimension for a given vector $Q = (Q_j)$ of outputs depended upon the set of output characteristics Q_j we have chosen to focus on. However, there is a natural way to define a flexibility dimension of the full system which accounts for the complete set of possible outputs in one go. This is because all changes in the output characteristics of importance are determined by the change in the limit cycle γ and its period τ. A small change δk in the parameters will cause a change $(\delta\gamma, \delta p)$ to the limit cycle γ and its period τ and the changes in all output variables can be calculated from these.

The limit cycle can be regarded as a function $\gamma : \mathbb{R} \to \mathbb{R}^n$ which is periodic with period τ: $\gamma(t + \tau) \equiv \gamma(t)$. Since, the period τ can vary with the parameters k it is necessary to normalize γ and replace it by

$$\tilde{\gamma}(t) = \gamma(\tau(k)t).$$

Then, as k varies, $\tilde{\gamma}$ remains periodic of period 1 and therefore the derivative $M^* : \delta k \to (\delta\tilde{\gamma}, \delta\tau)$ is a map from variations δk into the product of the space of functions of period 1 with $\mathbb{R}$. Clearly, $(\tilde{\gamma}, \tau)$ determines (γ, τ) and *vice-versa*. Thus we consider $M^* : \delta k \to (\delta\tilde{\gamma}, \delta\tau)$ rather than the correspondence $\delta k \to (\delta\gamma, \delta\tau)$.

Definition 4. The *flexibility dimension d* (of the system) is the largest dimension of any linear subspace that is contained in the accessible cone $C(k, \varepsilon)$ for $Q = (\tilde{\gamma}, \tau)$.

Note that if we are dealing with an entrained system the period τ does not change when the parameters are varied by a small amount. Therefore in this case we can ignore the variations $\delta\tau$.

Since we assume that the outputs are a function of the limit cycle and its period alone, for any given vector $Q = (Q_j)$ of outputs, the matrix M above is the form $M_p \cdot M^*$ where M^* is the above linear operator. The matrix M_p is the linearized relationship between the normalised change in the limit cycle $\delta\tilde{\gamma}$ plus change $\delta\tau$ in period and the particular output characteristics being

Table 2
Flexibility dimension and relevant singular spectrum of various published models

Model	n	s	d	$\log_{10} \sigma_j/\sigma_1$ with $\sigma_j/\sigma_1 > 10^{-2}$
Leloup et al. (1999) *Neurospora*	3	10	1, 1, 2, 3	0, −1.03, −1.22, −1.30, −1.78, −1.93
			1, 2, 3, 4	0, −0.97, −1.15, −1.26, −1.62, −1.75, −1.81
Leloup et al. (1999) *Drosophila*	10	38	1, 3, 3, 3	0, −0.69, −0.94, −1.68, −1.96
			2, 3, 3, 6	0, −0.19, −0.85, −1.32, −1.38, −1.43, −1.59
Ueda et al. (2001) *Drosophila*	10	55	1, 1, 1, 2	0, −1.21, −1.86, −1.99
			1, 1, 1, 2	0, −1.33, −1.52, −1.67, −1.84, −1.93
Leloup and Goldbeter (2003) mammal	16	53	2, 3, 3, 5	0, −0.30, −0.91, −1.34, −1.46, −1.61, −1.64, −1.75, −1.95
			1, 2, 2, 5	0, −0.71, −1.24, −1.4, −1.5, −1.71, −1.74, −1.78, −1.88
Forger and Peskin (2003) mammal	73	36	3, 4, 5, 7	0, −0.41, −0.64, −0.79, −1.14, −1.31, −1.35, −1.57, −1.65, −1.84, −1.91
			5, 7, 9,10	0, −0.14, −0.37, −0.58, −0.61, −0.67, −0.82, −1.07, −1.1, −1.32, −1.53, −1.61, −1.7, −1.83, −1.84, −1.99

n and s are, respectively, the number of dynamical variables and parameters. The four values given for d are, respectively, the values of the flexibility dimension d when $\varepsilon^2 = 0.05$, 0.01, 0.005 and 0.001 so that the first d principal components capture approximately 95%, 99%, 99.5% and 99.9% of the variance. Thus the third of these is the number of log σ_i which are greater than $(\log_{10} 0.005)/2 \approx -1.15$. The set of upper values of d for each model are for absolute changes, i.e., they do not take account of the size of the parameters being perturbed so that the singular values given are those for M^*. The lower values are for changes that are measured relative to the size of the corresponding parameter values and therefore the singular values are those for $M^* \cdot \Delta_k$ (see text). Usually the set of lower values are the most relevant. We note that almost universally s is bigger than d by an order of magnitude and that d grows roughly linearly with the loop complexity. The ratio s/d is lower for the last model, but in this case the number of parameters s has been kept unusually low by assuming several different parameters always have the same value.

considered and as such is well behaved and easy to calculate. Therefore the relationship described by M^* is the crucial one and we estimate d from M^*.

Important Example. If Q is the vector whose entries are the phases of all the maxima and minima of all mRNA and protein products and all amplitudes of the oscillations in these products, then M_p is easy to calculate. Suppose that the time at which the ith product is maximal (resp. minimal) is t_i^+ (resp. t_i^-). Let the limit cycle be given by $\gamma = (x_i(t))$ so that $x_i(t)$ is the time course of the ith product. Then the ith amplitude is given by the $A_i = x_i(t_i^+) - x_i(t_i^-)$ and the phase of the maximum (resp. minimum) of the ith product is given by ϕ_n^+/τ (resp. ϕ_n^-/τ) where τ is the period of the limit cycle. Thus $Q = (A_1, \ldots, A_n, \phi_1^+, \ldots \phi_n^+, \phi_1^-, \ldots \phi_n^-)$ and the linear transformation M_p is given by $M_p \cdot (\tilde{\gamma}, \tau) = (A, \Phi^+, \Phi^-)$ where

$$A = (\delta x_1(t_1^+) - \delta x_1(t_1^-), \ldots, \delta x_1(t_n^+) - \delta x_1(t_n^-)) \tag{6}$$

and

$$\Phi^{\pm} = \left(\frac{\delta\phi_1^{\pm}}{\ddot{x}_1(t_1^{\pm})}, \ldots, \frac{\delta\phi_n^{\pm}}{\ddot{x}_1(t_n^{\pm})}\right). \tag{7}$$

Thus we see that provided the curvatures $\ddot{x}_i(t_i^{\pm})$ are of order 1 then the flexibility of the limit cycle and that of the Q considered here will be very close.

In Section B.3 we explain how to approximate and numerically calculate M^*.

3.3. Inflexibility of circadian clock models

We have estimated d directly for a range of systems by numerically calculating M^* for these systems and then carrying out the singular value decomposition of $M^* \cdot \Delta_k$. These results are shown in Table 2. The flexibility dimension has been calculated using Theorem 2 above, i.e. by calculating the number of singular values σ_i of $M^* \cdot \Delta_k$ with $\sigma_i/\sigma_1 > \varepsilon$.

We find that all these systems are relatively inflexible in the sense that for small values of ε^2 of the order 10^{-3}–10^{-2} the flexibility dimension d is smaller than the number s of parameters by an order of magnitude. On the other hand, increasing the loop complexity generally causes d to increase proportionally.

3.4. Floquet exponents and decay of the singular spectrum

The local structure of the dynamics near to the limit cycle are largely determined by the Floquet multipliers. They are associated with the different rates of contraction onto the limit cycle (Guckenheimer and Holmes, 1983). For the clock systems considered here, (i) one multiplier is 1 (corresponding to the direction along the limit cycle), (ii) all others have modulus less than 1 (i.e. the limit cycle is attracting) and (iii) almost all of them have a very small modulus (corresponding to directions with very fast contraction onto the limit cycle). The inflexibility is due to (iii) because the flexibility dimension d is related to the number of Floquet multipliers λ for which $1/|\log\lambda|$ is small (of order ε).

Property (iii) is due to the loop structure of the clocks and the nature of protein degradation and modification because these determine the Floquet multipliers. It is therefore expected to be a general feature of regulatory networks. Although it is difficult to prove general results about how rapidly the multipliers decrease, it is clear that a large class of regulatory systems will have this property. What is important for this are the following characteristics: (a) one or more of the protein products in each loop has a degradation rate whose time average is not too small and (b) the forward and backward rates $k_i^+, k_i^- : P_i \rightleftharpoons P_{i+1}$ (typically corresponding to (de)phosphorylation) also have a time average that is $O(1)$ on a time scale of hours. This fact ensures that the product of all the multipliers is of the order $\exp(-r\tau)$ where τ is the period of the oscillator and r is the number of products in the loop. This product is therefore extremely small. A more detailed calculation is needed to show that only very few of the multipliers are larger than $O(\varepsilon)$.

3.4.1. Sources of flexibility

Relevant singular values (i.e. those with $\sigma_j/\sigma_1 > \varepsilon$) and the corresponding Floquet multipliers are often associated with specific structural or dynamical aspects. For example, as we discuss in the next section, the largest multipliers of the models considered here are usually associated with phase changes.

For a single loop the other obvious way to generate relevant multipliers is to have a topology and rate constants that ensure that under reasonable starting conditions the mean time before a protein is degraded is large (for example because it typically has to go through a series of modifications and their reverses before it is in a state where it can be targeted for degradation). Otherwise, all but one of the Floquet multipliers have very small modulus.

A interesting consequence of this observation is that the need for flexibility constrains the molecular structure. For example, it seems to imply an evolutionary advantage for selective degradation. The more products in a loop that are degraded the smaller the modulus of the Floquet multipliers and hence the less flexible the system. Since some degradation has to occur, this suggests that as few as possible of the protein products in a loop should be degraded at as low a rate as possible.

The number of these relevant multipliers is multiplied when loops are coupled and, in addition, new ones result from the coupling. To see the latter consider the case when the coupling is weak. There will typically be a

multiplier associated with the way in which perturbations of the relative phase of the two loops die away. As the coupling is increased this multiplier may become smaller or complex but it will usually remain relevant. Thus we see that the flexibility dimension is much less than and roughly proportional to the loop complexity.

3.4.2. Principal components

We show below in Section A.2 that, in the limit of $N \to \infty$, the principal components (e_j, v_j) of a set of output changes $\delta Q^{(\ell)}$ produced by N random parameter changes is given by the singular value decomposition of the matrix M'. Applying this to the case where $Q = (\tilde{\gamma}, \tau)$ we get a set of principal components (e_j, v_j). Like $\tilde{\gamma}$, the e_j are given by functions $e_j : \mathbb{R} \to \mathbb{R}^n$ which are periodic with period 1. We discuss how to numerically calculate these in Section B.3.

Definition 5. The (e_j, v_j) are called the *principal components of limit cycle variations*.

If the limit cycle is given by $x = \gamma(t)$, a phase change by an amount α produces $x = \gamma_\alpha(t) = \gamma(t + \alpha)$. Thus

$$\Gamma_\alpha(t) = \left.\frac{\partial}{\partial \alpha}\right|_{\alpha=0} \gamma_\alpha(t) = \gamma'(t)$$

represents an infinitesimal phase change. When each of the models in Table 1 is entrained by light, we find that the dominant principal component, of the limit cycle variation (e_1, v_1) (i.e. the one associated to the largest singular value σ_1) is such an infinitesimal phase change (see Fig. 3).

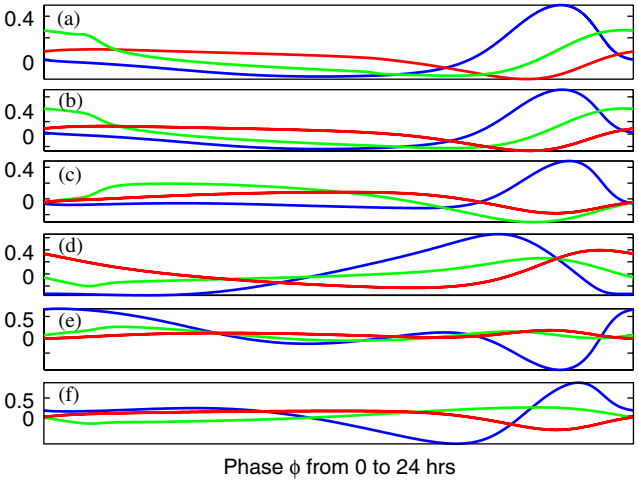

Fig. 3. (a) The derivative with respect to time of the limit cycle for the Drosophila model of Leloup et al. (1999). (b)–(f) the principal components with largest singular values for the matrix M^* for the same model. Only the *per* mRNA, phosphorylated TIM and nuclear PER:Tim complex levels are shown. The corresponding singular values are 1561.7, 318.1, 178.7, 32.6, 17.2. Note the similarity of the curves in (a) and (b) showing that the dominant principal component is an infinitesimal phase change.

This can be understood as follows. A general insight from the theory of dynamical systems is that those directions that a limit cycle moves most in when parameters are varied are correlated with the directions that are softest with respect to perturbations of the initial conditions, i.e., those directions with the property that a perturbation of the dynamical variables away from the limit cycle is least rapidly damped. These correspond to the direction associated with the Floquet multipliers (Guckenheimer and Holmes, 1983) of maximum modulus. This is shown in Section B.4. A perturbation of the dynamical variables causes a deviation away from the limit cycle, which is subsequently corrected. The correction has a rapid phase in which the shape of the limit cycle is recovered (so that $x = \gamma(t + \alpha)$) and a slow phase where the phase shift α is corrected. The way that this latter relaxation takes place will typically be described by one or two multipliers (Guckenheimer and Holmes, 1983): one when the coupling to light is relatively weak and the phase adjusts monotonely and two (as in the *Neurospora* model of Leloup et al. (1999), see Tables 1 and 2) when the phase correction overshoots and the multipliers are complex conjugates. Thus parameter changes easily result in a change of phase while other characteristics (such as phase relationships) are harder to change with the difficulty being greatest in systems with lower loop complexity.

3.4.3. Phase adjustments and homotopies to weak coupling

For each of the models considered we can express the parameters k_i as functions $k_i = k_i(\mu)$ of another parameter μ so that when $\mu = 1$ the parameter values are as in Table 1, when $\mu = 0$ the system is unforced by light (and therefore autonomous) and for all $0 < \mu \leqslant 1$ the system has a period τ_0 of 24 h and is entrained by light. This means that as μ is changed from 0 to 1 the one-parameter family of systems stays inside the 1/1 Arnold tongue (Guckenheimer and Holmes, 1983). Suppose the differential equation describing the model is given by $\dot{x} = g(t, x, k)$, $x \in \mathbb{R}^n$. For this part of the discussion it is useful to cast this into its equivalent form

$$\begin{aligned} \dot{y} &= g(\theta, y, k(\mu)), \\ \dot{\theta} &= 1, \end{aligned} \tag{8}$$

because this is an autonomous ordinary differential equation and therefore generates a dynamical system in $\mathbb{R}^n \times \mathbb{R}$. When $\mu = 0$ the system has a invariant torus $T_0 = \gamma_0 \times S^1$ where γ_0 is the limit cycle of the system $\dot{y} = g(\theta, y, k(0))$ (which does not depend upon θ when $k = k(0)$). This torus is normally hyperbolic (Guckenheimer and Holmes, 1983) since the limit cycle is hyperbolically attracting and therefore, as μ is increased from 0, while μ is small the torus persists in

the sense that it is deformed into a nearby attracting invariant torus T_μ. Since these systems are within the Arnold tongue, T_μ contains an attracting limit cycle γ_μ. Let $\gamma_\mu(s)$ denote the point $\gamma_\mu \cap \{\theta = s\}$. The tangent vector v_s to the intersection of T_μ with $\{\theta = s\}$ is an eigenvector of $Y(s, s+\tau_o)$ with eigenvalue $\lambda_\tau = 1 - O(\mu)$ close to 1. Thus if the other eigenvalues are much closer to zero (as is the case for the systems in Table 1) the sum in Eq. (B.20) giving $(\partial\gamma_k/\partial k_i)(t)$ is dominated by the term $(\lambda_\mu - 1)^{-1} v_t \int_t^{t+\tau_0} \mathrm{e}^{\chi(t+\tau_0-s)} b_{i,k}(s)\,\mathrm{d}s$ where $\chi = \log \lambda_\mu$ is close to 0. It can be seen then that the dominant principal component $\phi_1(s)$ (see above) is very close to being a infinitesimal phase shift of the original limit cycle $\gamma_\mu : y = \sigma_\mu(t)$, i.e.

$$\phi_1(s) \approx \frac{\mathrm{d}}{\mathrm{d}t}\,\sigma_\mu(s+t)\bigg|_{t=0} = \sigma'_\mu(s).$$

As μ is changed further towards 1, we can expect to see bifurcations of the form shown in Fig. 21 of Ostlund et al. (1983). As λ_μ moves away from 1, it may collide with another smaller eigenvalue. Until this happens we are essentially in the case discussed in the last paragraph. Near to where such a collision takes place we can restrict attention to the centre manifold determined by λ_μ and the eigenvalue it is going to collide with (assuming the other eigenvalues remain away from this pair). It is the dynamics on this two-dimensional centre manifold that should be compared with the above-mentioned bifurcations. We expect that when λ_μ collides with another eigenvalue they will produce a pair of complex conjugate eigenvalues λ_μ and $\bar{\lambda}_\mu$. When this happens the one-dimensional eigenspace given by v_s is replaced by a two-dimensional eigenspace V_s and one can show that the two dominant principal components $\phi_1(s)$ and $\phi_2(s)$ are dominated by $\sigma'_\mu(s)$ and $\sigma''_\mu(s)$.

4. Infinitesimal response curves

We now turn to consider the key question above about evolution seeking to simultaneously tune multiple characteristics: to what extent can the key characteristics be tuned independently and which of them are strongly related. In particular, we would like to describe which combinations of parameters can be tuned in order to produce a specific circadian characteristic. The aim is to characterize the key evolutionary goals so that they are given by transparent and comparable mathematical conditions. Again we make use of the fact that the effect of small parameter changes can be well approximated using perturbation theory. The quality of approximation can be determined by calculation of higher-order terms.

Our main tools are what we call *infinitesimal response curves*. We consider the linear approximation to the change δQ_j produced by a small change δk_i of the parameter k_i. An infinitesimal response curve for Q_j and k_i tells us how different phases of the oscillation contribute to δQ_j.

Suppose that our oscillator has a stable limit cycle $\gamma = \gamma_k$ of period τ given by $x = g(\phi)$ with ϕ representing the phase, i.e. time t mod τ. A key insight is that for each parameter k_i and each output Q_j there is a function $f_{k_i,Q_j}(\phi)$ of the phase ϕ such that if one changes $(k_1, \ldots, k_s)$ to $(k_1 + \delta k_1, \ldots, k_s + \delta k_s)$ only when the phase ϕ is between ϕ_1 and ϕ_2 (not necessarily close together), the linear approximation to the change δQ_j in a output variable Q_j is of the form

$$\delta Q_j = \sum_{i=1}^{s} \delta k_i \cdot \left(\int_{\phi_1}^{\phi_2} f_{k_i,Q_j}(\phi)\,\mathrm{d}\phi \right) + O(\|\delta k^2\|). \tag{9}$$

Theorem 6. *For each parameter k_i and each output Q_j which is a function of the limit cycle γ and its period τ, there is a unique function $f_{k_i,Q_j}(\phi)$ of the phase ϕ such that Eq. (9) holds for all choices of ϕ_1 and ϕ_2.*

Definition 7. The function $f_{k_i,Q_j}(s)$ is called the *infinitesimal response curve* (IRC) of variable Q_j on parameter k_i.

We give formulas for these IRCs and a proof of Theorem 6 in Appendix B. Using these the IRCs can be numerically computed very rapidly from their analytical expressions for all parameters and all relevant output variables. Fig. 4 shows the largest amplitude IRCs for a model of the Drosophila clock when Q_j is period.

Recall the definition of the normalized limit cycle $\tilde{\gamma}$ given in Section 3.2.2: if $x = \gamma(t)$ is the limit cycle and $\tau = \tau(k)$ is its period then $\tilde{\gamma}(t) = \gamma(\tau(k)t)$. In what follows we are going to use the fact that any such small change δQ_j is a linear function of the normalised change $\delta\tilde{\gamma}$ in the limit cycle (see Section 3.2.2) and the change $\delta\tau$ in the period: $\delta Q_j = M^* \cdot (\delta\tilde{\gamma}, \delta\tau)$.

4.1. IRCs and phase response curves (PRCs)

When Q_j is the period of the cycle for a free-running clock

$$f(\phi) = -\delta k_i \cdot \int_{\phi_1}^{\phi_2} f_{k_i,Q_j}(\phi)\,\mathrm{d}\phi + O(\|\delta k\|^2) \tag{10}$$

is the phase response curve (PRC) (Winfree, 2001) of a small perturbation δk_i in the parameter k_i applied between the phases ϕ_1 and ϕ_2. This follows from the Lemma of Section B.5. We are using the fact that at the infinitesimal level the change in period $\mathrm{d}\tau$ is minus the change in phase $\mathrm{d}s$.

If this change in k_i is caused by light then Eq. (10) gives an approximation to the usual phase response curve for a light pulse applied between the phases ϕ_1 and ϕ_2. Thus, since for the models under consideration the curves given by Eq. (10) provide excellent approximations to the usual PRCs even when the

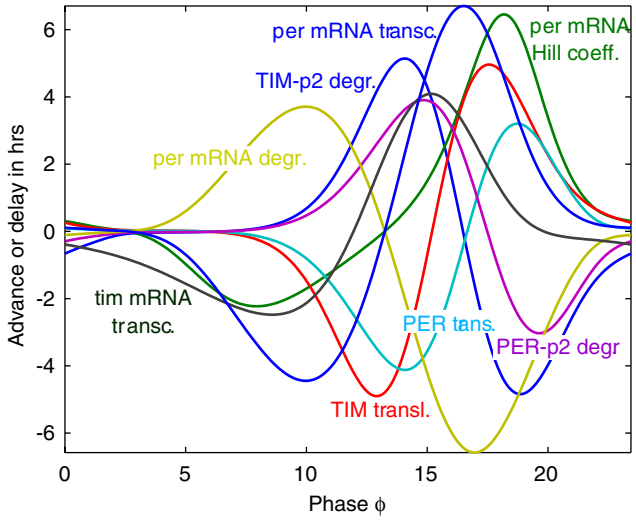

Fig. 4. This shows all the large amplitude IRCs $f_{k_i,period}(\phi)$ for period for the *Drosophila* model of Leloup et al. (1999).

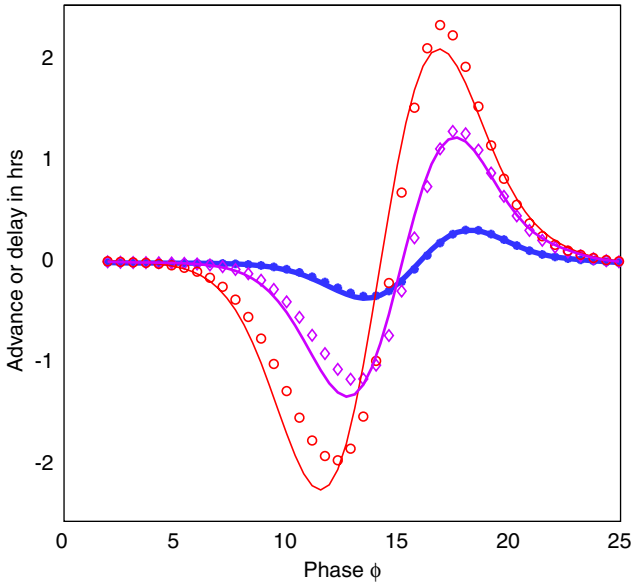

Fig. 5. PRCs for the Drosophila model of Leloup et al. (1999) for light pulses duration 1 (blue stars), 2 (purple triangles) and 4 h (red circles) together with the approximation of them by integrating the corresponding IRC (as given in Eq. (10)) from dawn to dusk (corresponding colour solid curve). The PRCs are calculated directly by simulating the system. In this model light acts by increasing the degradation of TIM-p2 and thus the IRC used in the integral is $-f_{v_{dt},period}(\phi)$ because the parameter v_{dt} is changed when light is on. The effect of the light is as in the original publication (v_{dT} is changed from 3 to 6nMh-1) but we very slightly changed the light profile by smoothing out the discontinuities.

perturbations δk_i are not particularly small (see Fig. 5), the analytical expressions allow rapid computation of all possible PRCs without having to simulate the system and calculate PRCs in the usual way.

Using the results of an analysis such as that shown in Fig. 4, one can estimate the effects of any hypothetical input pathway on the phase and strength of entrainment (see next section). Moreover, it follows from the linearity of Eq. (9) that one can also estimate the effect of combinations of different pathways by simply adding them together with the appropriate weights. We will also show below that via Eq. (9) such an analysis gives key insights into stability, and temperature and pH compensation.

5. Evolutionary aims and IRCs

In the discussions that follow the linear nature of the relationship in Eq. (9) will play a crucial role because it allows us to combine changes to multiple parameters by simply adding them together with the appropriate weights. Thus, for example, if light of intensity I acts by changing k_i and k_j by amounts $\delta k_i(I)$ and $\delta k_j(I)$ between ϕ_1 and ϕ_2 then the combined (infinitesimal) phase response curve is given by

$$f(\phi) = -\int_{\phi_1}^{\phi_2} (\delta k_i(I)\cdot f_{k_i,period}(\phi) + \delta k_j(I)\cdot f_{k_j,period}(\phi))\,\mathrm{d}\phi. \tag{11}$$

5.1. Entrainment

To consider how entrainment can be discussed in terms of IRCs we return to the earlier discussion of Section 2.1. We consider the situation where light of intensity I acts for a time interval of duration S from dawn to dusk. We suppose that this light acts by changing the parameter k_i to $k_i + \delta k_i(I)$. If the phase at dawn of the nth day is ϕ_n then at dusk it is $\phi_n + S + \Phi(\phi_n)$ where

$$\Phi(\phi) = -\delta k_i(I)\int_{\phi}^{S+\phi} f_{k_i,period}(t)\,\mathrm{d}t \tag{12}$$

provided that the linear approximation is valid. Therefore at the end of the day the phase is given by

$$\phi_{n+1} = F(\phi_n) = \phi_n + \Phi(\phi_n) + (L-\tau). \tag{13}$$

If there are multiple input pathways then one can use the analogue of Eq. (11) to combine them. For each parameter k_i affected by light one obtains a function Φ_i as in Eq. (12) and then just adds them to get $\Phi = \sum_i \Phi_i$.

As discussed in Section 2.1, entrainment corresponds to the existence of a stable fixed point ϕ_* of the map F given by Eq. (13) because then, for almost all starting conditions ϕ_0, the system eventually settles down to a state where ϕ_n is approximately constant at ϕ_* ($\phi_n \to \phi_*$ as $n \to \infty$). A fixed point ϕ_* satisfies the equation $\Phi(\phi_*) = \tau - L$. If the graph of F is drawn (as in

Fig. 6), the fixed points correspond to the intersections between the graph and the diagonal given by $\phi_{n+1} = \phi_n$. The fixed point (and hence entrainment) is stable provided $-1 < \Phi(\phi_*) < 0$ because then $|F'(\phi_*)| < 1$.

Robustness of the entrainment means that the stable fixed point of F persists under reasonable environmental, physiological and other perturbations. Thus entrainment requires that the amplitude of Φ is greater than the circadian correction $L - \tau$. Otherwise, there will be no intersection between the graph of the map F and the diagonal given by $\phi_{n+1} = \phi_n$. However, it follows that, since Φ is approximately given by Eq. (12), entrainment can only occur if $\delta k_i(I) f_{k_i,period}$ has sufficient amplitude to produce a phase shift of $L - \tau$ (Johnson et al., 2003). The required amplitude as a function of $L - \tau$ can be estimated from Eq. (13). Moreover, the fixed point ϕ_* determines the phase of entrainment and this can be determined from $f_{k_i,phase}$ in the same manner as from a PRC.

Although this relationship is only approximate it is very informative and, for example, as we see in the next section, it allows us to study the relationship between robust entrainment by a given environmental variable and robustness of the period to sustained changes in that variable.

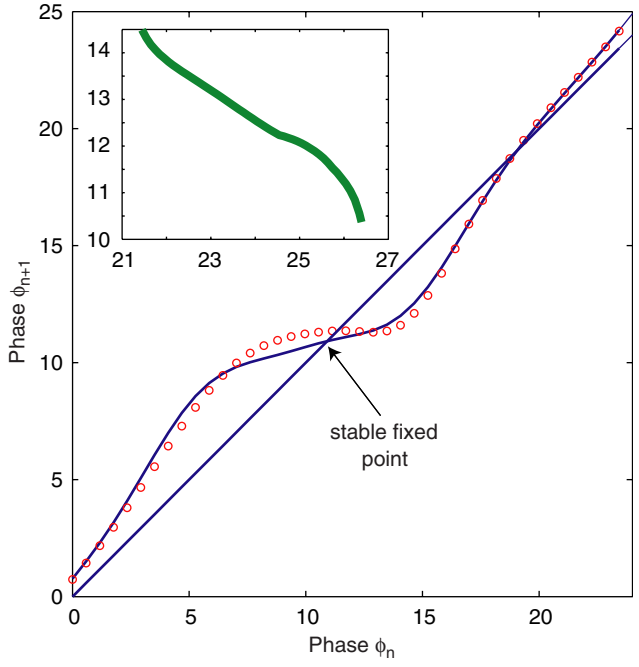

Fig. 6. The phase return mapping F for the *Drosophila* model of Leloup et al. (1999) when the day length is 9 h. The solid line shows the mapping as calculated using the IRCs as in Eq. (12) and the circles show the mapping using the numerically calculated PRC. The embedded graph shows the phase of entrainment as a function of the period τ of the unforced system calculated using the mapping (solid line) and directly (dots). The period τ was changed using a numerical tool that we have developed that allows one to move parameters so as to change a particular output (here τ) without changing the other key outputs.

5.2. Temperature compensation

As noted above circadian clocks are *temperature compensated* in that they maintain a roughly constant period over a relatively wide range of temperatures (Rensing and Ruoff, 2002). Temperature T will presumably affect a number of parameters k_i which will be functions of $T : k_i = k_i(T)$. When temperature changes from T to $T + \delta T$ then the change in the parameter k_i will be approximated by $k_i'(T) \cdot \delta T$ where $k_i'(T)$ is the derivative of $k_i(T)$. Thus by the linearity of Eq. (9) we can define the IRC for temperature (at T) acting on the output variable Q_j by

$$f_{T,Q_j}(\phi) = \sum_i k_i'(T) f_{k_i,Q_j}(\phi).$$

Then temperature compensation holds around T provided the integral of over a complete cycle is close to zero (Ruoff, 2000):

$$\int_0^\tau f_{T,Q_j}(\phi)\,\mathrm{d}\phi \approx 0. \tag{14}$$

By Eq. (9) the change in Q_j caused by such a temperature change is given by

$$\begin{aligned}\delta Q_j &= \delta T \cdot \sum_{i=1}^{\phi} k_i'(T) \cdot \int_0^\tau f_{k_i,Q_j}(\phi)\,\mathrm{d}\phi + O(\|\delta T^2\|) \\ &\approx \delta T \int_0^\tau f_{T,Q_j}(\phi)\,\mathrm{d}\phi.\end{aligned}$$

The chief advantages of IRCs in this context are (a) that the effects of multiple parameter changes are very easy to compute and (b) that using the discussion about the relationship between entrainment and IRCs in Section 5.1 and the discussion here we can relate temperature compensation and the entrainment properties of temperature.

A commonly considered functional form for the temperature dependence of a reaction is given by the Arrhenius relation:

$$k_i = A_i \exp\left(-\frac{E_i}{RT}\right), \tag{15}$$

where A_i is the so-called pre-exponential factor, E_i is the activation energy of the reaction and R is the gas constant. In this case $k_i'(T) = k_i E_i / RT^2$ and, if $I_i = \int_0^\tau f_{k_i,Q_j}(\phi)\,\mathrm{d}\phi$, then condition (14) is equivalent to

$$\sum_i k_i E_i I_i \approx 0 \tag{16}$$

as derived in Ruoff (2000). In Fig. 7, we show an example of a temperature compensated system that satisfies Eq. (16).

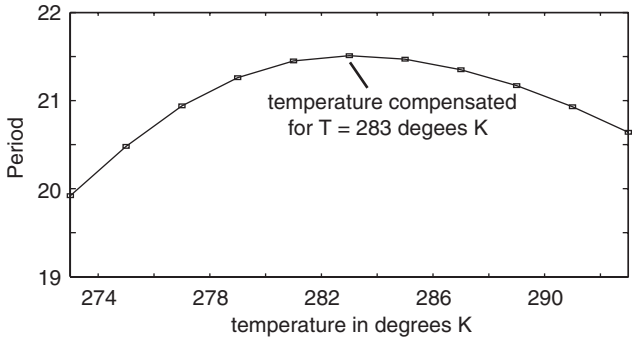

Fig. 7. In this figure we have chosen the activation energies E_i so that the Leloup-Goldbeter model for *Neurospora* (Leloup et al., 1999) is temperature compensated at $T = 283$. The relation between k_i and T is given by Eq. (15). We see that near to $T = 283$ the period changes slowly with T but further away it changes more rapidly. Biological oscillators have a more global temperature compensation where the period is roughly constant over a more substantial temperature range. Thus we refer to this as global temperature compensation and the sort seen in the figure as local temperature compensation. We will discuss how to achieve global compensation in a later paper.

At first sight entrainment by temperature and temperature compensation can appear at loggerheads. We can, however, see that this is not the case. Robust entrainment requires that $\Phi(\phi) = \int_{\phi}^{L+\phi} f_{T,period}(\sigma)\,\mathrm{d}\sigma$ does not have a small amplitude so that the stable solution to $\Phi(\phi) = \tau - L$ is relatively robust while temperature compensation requires that $\int_0^{\tau} f_{T,period}(\phi)\,\mathrm{d}\phi \approx 0$. Therefore these are perfectly compatible goals.

5.3. Robustness to parameter perturbations

If we require that the period or other output variable Q_j is relatively stable to perturbations of the parameter k_i then by Eq. (9) we require that the integral over a complete cycle in Eq. (9) of the IRC is close to zero:

$$\int_0^{\tau} f_{k_i,Q_j}(\phi)\,\mathrm{d}\phi \approx 0. \tag{17}$$

By the linearity of Eq. (9) we can apply this to study mixed perturbations of many parameters. Robustness to sustained parameter perturbations requires that all IRCs must have very small integral as in Eq. (9). We can ignore those IRCs that have small amplitude because they will therefore have small integral. However, by the above, some IRCs must have large amplitude for entrainment to be possible and, as in the models considered in Table 1, for some other parameters k_i and output quantities Q_j the IRCs will have large amplitude because of the nature of k_i and Q_j (e.g. for the effect of phosphorylation and degradation rates on period). It is widely thought that there is a strong evolutionary advantage to robustness, so selection may be expected to change the system so as to balance the large amplitude IRCs so that their integral is small. This provides a significant number of evolutionary goals.

5.4. Output pathways amplitudes and phases

We consider a particular output pathway driven by the molecular species whose level is given by $x_i(t)$. The change in the level of $x_i(t)$ at $t = t_0$ produced by a small change in the parameters can be calculated directly from the IRCs f_{k_i,Q_j} where $Q_j = x_i(t_0)$ via Eq. (9).

If we want to track the phase s of the minimum or maximum of $x_i(t)$ we can proceed as follows. The phase $s = s(k)$ satisfies $\dot{x}_i(s) = 0$ or equivalently $g_i(s, x(s), k_0) = 0$ where $\dot{x}_\ell = g_\ell(t, x, k)$, $\ell = 1, \ldots, n$ is the system under consideration. Differentiating this relationship with respect to k_j and solving for $\partial s/\partial k_j$ gives

$$\frac{\partial s}{\partial k_j} = \left(\sum_\ell \frac{\partial g_i}{\partial x_\ell}\cdot g_\ell\right)^{-1}\left(\frac{\partial g_i}{\partial t} + \sum_\ell \frac{\partial g_i}{\partial x_\ell} \cdot\left[\frac{\partial x_\ell}{\partial x_\ell^0}\frac{\partial x_\ell^0}{\partial k_j} + \frac{\partial x_\ell}{\partial k_j}\right] + \frac{\partial g_i}{\partial k_j}\right), \tag{18}$$

where x^0 is the initial point on the limit cycle that is the initial condition. In this expression derivatives of g_i and g_ℓ are evaluated at $x = x(s_0, k_0)$, $s = s_0$ and $k = k_0$, derivatives of x_ℓ are evaluated at $x = x^0$, $s = s_0$ and $k = k_0$, and the derivatives of x_ℓ^0 at $k = k_0$.

The derivatives $\partial x_\ell/\partial x_\ell^0$ are given by the matrix solution $Y(t)$ of either Eq. (B.3) or Eq. (B.14) in Appendix B and those of $\partial x_\ell^0/\partial k_j$ are given by integrating the IRC f_{k_ℓ,x^0} where x^0 is the point on the limit cycle at the starting phase.

5.5. Robustness to stochastic perturbations

It is worthwhile considering this in the context of the large Ω limit where Ω is the number of molecules involved in the clock (Gonze et al., 2002). In this limit the fluctuations about the limit cycle are normally distributed with zero mean. After N cycles of the period T the projections of these fluctuations onto the direction of the limit cycle (i.e. the fluctuations in the time to complete N oscillations) have a variance that is $\sigma^2 = N/\alpha\Omega$ where α is calculated according to the prescription in Gonze et al. (2002).

The projections onto the eigendirection that are transverse to the limit cycle (the directions $z_j(t)$ of Section B.4) have a variance that is $O(|\rho_j|^2)$ where ρ_j is the corresponding eigenvalue. It follows from this that one can often reduce the effect of stochastic perturbations by reducing the eigenvalues. However, this also reduces the flexibility of the system. Therefore, evolution must trade off these two effects or come up with different ways of counteracting this stochasticity.

6. Discussion and future prospects

We have presented an analysis of key evolutionary aims of circadian clocks such as robustness to perturbations, temperature and pH compensation, appropriate period, robust entrainment by environmental signals, and correct phase relationships for output pathways. It is widely believed that there is selective pressure for each of these targets. We have discussed the characterization of each of these targets in terms of IRCs (see Table 3). These IRCs are relatively easy to calculate and we have provided software to do this on our website. We have discussed in detail the mathematical theory behind IRCs and described in detail how they can be computed numerically. The underlying perturbation theory for periodic orbits is classical but we give a new way of looking at this which is particularly useful in the context of circadian rhythms. Our analysis of the mathematical characterization of these aims in terms of the tuning of output quantities expressed in terms of IRCs is summarized in Table 3.

The IRCs for period give accurate approximations of PRCs for environmental pulses with a broad range of durations and intensities via Eq. (9). We have explained the mathematical theory underlying this results in Appendix B (e.g. in Section B.5). This can be used to study entrainment by environmental signals such as light or temperature.

We find that robust entrainment requires that the appropriate combination of IRCs for the pathways involved in the environmental input has large amplitude and that the circadian correction $L-\tau$ is appropriate to ensure a robust stable fixed point of the mapping F given by Eq. (13). On the other hand properties like temperature compensation require that the IRC for temperature, which is a linear combination of basic IRCs $f_{k_i,period}$ is balanced in the sense of Eq. (14). A similar argument applies to compensation for sustained variations of other environmental components such as pH. Thus we see that the conditions for robust entrainment by an environmental variable such as temperature and compensation for that variable are independent and perfectly compatible. Stability of key output variables with respect to parameter changes is also characterized by Eq. (17). This suggests that for key outputs Q_j it will be necessary for evolution to roughly balance (in the sense of Eq. (17)) those IRCs which have large amplitude because otherwise these outputs will be unstable to variations in the parameters. For example, if Q_j is period and f_{k_i,Q_j} has large amplitude and is far from balanced then sustained variations in k_i are likely to change the circadian correction sufficiently to destroy entrainment (see Fig. 6 and Eq. (13)). The conditions for correctly tuned output pathways and the robustness of this correct tuning also involve combinations of the IRCs.

Since we can express the various evolutionary aims in terms of IRCs we can determine to what extent they are independent of each other. This requires an analysis of which IRCs are involved, the nature of the condition on the IRC and the extent to which the IRCs are linearly independent of each other. However, it is not difficult to see that in general a large number of the most important evolutionary goals discussed here are independent. It therefore emerges that there are multiple independent characteristics that we can expect will confer a selective advantage and moreover that should be accessible to a process of small random perturbations and selection provided the flexibility of the clock is large enough. It seems reasonable that, there will be more than 5 or 6 such characteristics that are of key importance and therefore that the flexibility needed to achieve this will at least require a loop complexity equivalent to the most loop complex models in Table 1.

In order to simultaneously tune q of the characteristics that are of key importance it is necessary to be able

Table 3
Summary of how different properties are characterized by IRCs

Evolutionary aim	Mathematical characterization in terms of IRCs
Setting period	change in period $Q_j=\tau$ due to change δk_i is $\delta k_i \int_0^\tau f_{k_i,period}(\phi)\,d\phi$
Entrainment	stability and phase determined by $V(\psi)=-\delta k_i(I)\int_\psi^{L+\psi} f_{k_i,period}(\phi)\,d\phi$ when input pathway modulates k_i
PRCs for short disturbances of duration $d\phi$	PRC Q_j approximated by $-\delta k_i \cdot f_{k_i,period}(\phi)\,d\phi$ when input pathway modulates k_i
PRCs for disturbances lasting for an interval S and starting at phase ψ	PRC Q_j approximated by $-\delta k_i(I)\int_\psi^{S+\psi} f_{k_i,period}(\phi)\,d\phi$
Temperature compensation	$Q_j=\int_0^\tau f_{T,Q_j}(\phi)\,d\phi\approx 0$
pH compensation	$Q_j=\int_0^\tau f_{pH,Q_j}(\phi)\,d\phi\approx 0$
Parameter stability for k_i	$Q_j=\int_0^\tau f_{k_i,Q_j}(\phi)\,d\phi\approx 0$
Phase relationships for $x_i(t)$	uses $f_{\mu_i,\gamma_i,t}(s)$

Each evolutionary aim can be described as tuning one or more particular output variables Q_j. Note that in the case of entrainment and PRCs, Q_j is actually a function rather than just a number.

to move the appropriate output vector Q independently in q dimensions by using small changes in the parameters. However, even if one can freely move lots of parameters it does not follow that by doing this one can freely move the output Q with the same dimensionality. Movement of Q in certain directions is highly resisted for the clock systems studied. Seen another way: if the parameter changes are random and uncorrelated then the movement produced in Q will tend to be highly correlated with the changes strongly concentrated in just a few dimensions. The number d of these dimensions is given by the flexibility dimension that we have defined. We have shown that this flexibility dimension is given by the singular values of the matrix M^* and have rigorously related the two approaches to flexibility.

We have provided strong evidence that the flexibility dimension d is smaller than the number of parameters by an order of magnitude and roughly proportional to the loop complexity of the system. Thus evolution will only be effective in reaching multiple independent targets if the flexibility dimension d of the system is as large as the number of targets. If the system is constrained so that it can only reasonably move in a small number of dimensions then it will only be able to tune a small number of targets.

It follows that there is likely to be a strong selective advantage in increasing loop complexity and strong selection for mechanisms that enable this such as gene duplication and protein variation. Mechanisms and divergence that may increase complexity are found in the circadian clocks of *Neurospora* (Garceau et al., 1997), *Drosophila*, *Arabidopsis* (Eriksson et al., 2003) and the mouse (Daan et al., 2001; Zheng et al., 2001; Oster et al., 2002). In addition, we have argued that the selective degradation of protein products also aids flexibility and therefore that we would expect to find that not all protein products are degraded at the same rate but that degradation is concentrated on selected products in certain modified states.

Since one can understand the lack of flexibility in terms of properties of dynamical systems one can make some estimate of the range of applicability of these ideas. It therefore seems rather clear that the ideas discussed will apply to a broad range of dynamical processes of such regulatory networks and not just to oscillating systems. For example, similar ideas should apply to the propagation of perturbations along pathways, multistable networks that act, for example, as switches and networks of transcription factors that determine spatial patterning.

Acknowledgments

We are grateful to Hugo van den Berg, Sanyi Tang, Ozgur Biringen-Akman and Isabelle Carré for useful discussions on these topics. Financial support was provided by the BBSRC and EU (BioSim Network Contract No. 005137). Correspondence and requests for materials should be addressed to: D. A. Rand, University of Warwick, Coventry CV4 7AL, UK, email: dar@maths.warwick.ac.uk

Appendix A. Proofs of results relating flexibility and singular values

A.1. Proof of Theorem 2

Let $M' = UDV^t$ be the singular value decomposition of M' where $D = \mathrm{diag}(\sigma_1, \ldots, \sigma_s)$ and we order the $\sigma_j > 0$ so that $\sigma_1 \geqslant \sigma_2 \geqslant \cdots \geqslant \sigma_s$. Let u_j and v_j denote, respectively, the columns of U and V corresponding to σ_j. Then $M' \cdot v_j = \sigma_j u_j$ and therefore, if $v = \sum_j a_j v_j$, $u = M' \cdot v = \sum_j a_j \sigma_j u_j$. Moreover, since the v_j (resp. u_j) are orthonormal, $\|v\|^2 = \sum_j a_j^2$ and $\|u\|^2 = \sum_j a_j \sigma_j^2$. It follows immediately from this that $R^* = \sigma_1$.

Every δQ in the image of M' can be written as $\sum_j a_j u_j$ where the sum is over those j where $\sigma_j \neq 0$. Then $\|\delta Q\|^2 = \sum_j a_j^2$. Moreover, if $\delta\eta = \sum_j \sigma_j^{-1} a_j v_j$, $M' \cdot \delta\eta = \delta Q$. If this sum is only over those j with $\sigma_j/\sigma_1 > \varepsilon$ then if follows that $\sigma_1^2 \|\delta\eta\|^2 = \sum_j (a_j \sigma_1/\sigma_j)^2 \leqslant \varepsilon^{-2} \sum_j a_j^2 = \varepsilon^{-2} \|\delta Q\|^2$ and therefore δQ is in the cone $C(\varepsilon, k)$. Therefore, since, $R^* = \sigma_1$, $C(\varepsilon, k)$ contains the vector space W spanned by the u_j with $\sigma_j/\sigma_1 > \varepsilon$.

Now suppose that W_1 is a linear subspace contained in the cone and of maximal dimension. Let $\pi : W_1 \to W$ be the projection

$$\pi\left(\sum_j a_j u_j\right) = \sum_{j:\sigma_j/\sigma_1 > \varepsilon} a_j u_j.$$

The kernel of π consists of vectors of the form $\delta Q = \sum_j a_j u_j$ where the sum is only over those j such that $0 < \sigma_j/\sigma_1 \leqslant \varepsilon$. Let $\delta\eta = \sum_j (a_j/\sigma_j) u_j$ so that $M' \cdot \delta\eta = \delta Q$. Then, since $\sigma_1^2 \|\delta\eta\|^2 \geqslant \varepsilon^{-2} \|\delta Q\|^2$ the vector δQ is not in the cone. Since W_1 is in the cone it follows that $\ker \pi = 0$ and therefore that the dimensions of W_1 and W are the same. Thus the dimension of W_1 is equal to the number of singular values with $\sigma_j/\sigma_1 > \varepsilon$.

A.2. Proof of Theorem 3 relating the principal components, the SVD of M' and the cone $C'(\varepsilon, k)$

As above $M' = UDV^t$ is the singular value decomposition of M', u_j denotes the j'th column of U, $m = \dim \delta Q$ and $D = \mathrm{diag}(\sigma_1, \ldots, \sigma_m)$ is the matrix of singular values (see Section 3.2.1).

Lemma A.1. *If the components $\delta\eta_i^{(\ell)}$ of the vector $\delta\eta^{(\ell)}$ are independent with variance Σ^2 then in the limit $N\to\infty$, $v_i\to\Sigma\sigma_i$ and $e_j\to u_j$.*

Proof. Firstly we note that the principal components (e_j, v_j) associated with Y are given by the singular value decomposition $A = U_A D_A V_A^t$ of A. In fact, the e_j are the columns of U_A and $v_j^2 = \kappa_j^2/N$ where the κ_j are the diagonal elements of D_A. This follows because $\mathbf{Y} = N^{-1}AA^t = U_A(N^{-1}D_A^2)U_A^t$.

Now we show that as $N\to\infty$, $v_i\to\Sigma\sigma_i$ and $e_j\to u_j$. Let us write the vectors $\delta\eta^{(\ell)}$ in the basis given by the vectors v_j which are the column of V above so that $\delta\eta^{(\ell)} = \sum_j a_j^{(\ell)} v_j$. Then $M'\cdot\delta\eta^{(\ell)} = M'V\mathbf{a}^{(\ell)} = UD\mathbf{a}^{(\ell)}$ where $\mathbf{a}^{(\ell)}$ is the (column) vector $(a_1^{(\ell)},\dots,a_m^{(\ell)})^t$, $m = \dim\delta Q$.

Let $\mathbf{a}$ be the matrix whose ℓth column is $\mathbf{a}^{(\ell)}$. Then the matrix A above is given by $UD\mathbf{a}$ so that $\mathbf{Y} = UDCDU^t$ where $C = N^{-1}\mathbf{a}\mathbf{a}^t$. The entries of this latter matrix are the correlations $C_{ij} = N^{-1}\sum_{\ell=1}^N a_i^{(\ell)}a_j^{(\ell)}$. Therefore, if we assume that the components $\delta\eta_i^{(\ell)}$ of the vector $\delta\eta^{(\ell)}$ are independent with variance Σ^2 we have that in the limit $N\to\infty$, $C = \Sigma^2 I$ where I is the identity matrix. This follows because if $\mathbf{a} = X\cdot\delta\eta$ with X an orthonormal matrix (as is the case here), then $N^{-1}\sum_{\ell=1}^N a_i^{(\ell)}a_j^{(\ell)}\to\delta_{ij}\Sigma$ as $N\to\infty$. Thus, as $N\to\infty$, $\mathbf{Y}\to U\Sigma^2D^2U^t$ so that $e_j\to u_j$ and $v_i\to\Sigma\sigma_i$. □

Now we relate all this to the cone $C'(\varepsilon,k)$ defined in Eq. (5).

Lemma A.2. *If $v = \sum_j b_j u_j$ is any vector in the image of M' and the $\delta\eta^{(\ell)}$ and $\delta Q^{(\ell)}$ are as in Lemma* A.1, *then*

$$\lim_{N\to\infty} N^{-1}\sum_\ell(\delta Q^{(\ell)}\cdot v)^2 = \Sigma^2\sum_j\sigma_j^2 b_j^2$$

and

$$\lim_{N\to\infty} N^{-1}\sum_\ell(\delta Q^{(\ell)}\cdot\delta Q^{(\ell)}) = \Sigma^2\sum_j\sigma_j^2.$$

Proof. As in the previous proof let $\delta\eta^{(\ell)} = \sum_j a_j^{(\ell)}v_j$ so that $\delta Q^{(\ell)} = M'\cdot\delta\eta^{(\ell)} = \sum_j\sigma_j a_j^{(\ell)}u_j$. Then

$$N^{-1}\sum_\ell(\delta Q^{(\ell)}\cdot v)^2 = \sum_j\sigma_j^2 b_j^2 C_{jj} + \sum_{j\neq k}\sigma_j\sigma_k b_j b_k C_{jk},$$

where $C_{jk} = N^{-1}\sum_\ell a_j^{(\ell)}a_k^{(\ell)}$ is the correlation discussed in the proof of Lemma A.1.

The first part of the lemma then follows from the fact that $C_{jk}\to\delta_{jk}\Sigma$ as $N\to\infty$. The second part follows immediately from this fact and the expression for $\delta Q^{(\ell)}$ in terms of the $a_j^{(\ell)}$. □

Corollary A.3. *A vector $v = \sum_j b_j u_j$ lies in the cone $C'(\varepsilon,k)$ if and only if $(\sum_j\sigma_j^2 b_j^2)/(\sum_j b_j^2)(\sum_j\sigma_j^2) > \varepsilon^2$.*

The proof of Theorem 3 follows from this.

Proof of Theorem 3. The proof is along the same lines as that of Theorem 2. One firstly uses Corollary A.3 to show that the vectors u_j with $\sigma_j^2 > \varepsilon^2\Xi$ are contained in the cone. Then one considers a linear subspace W_1 in the cone of maximal dimension and the projection π as in the proof of Theorem 2. Then the kernel of π consists of vectors of the form $\delta Q = \sum_j a_j u_j$ where the sum is only over those j such that $\sigma_j^2\leqslant\varepsilon^2\Xi$. For such a vector

$$\begin{aligned} R_{\delta Q}^2 &= \lim_{N\to\infty}\frac{\sum_\ell\langle\delta Q^{(\ell)},\delta Q\rangle^2}{\|\delta Q\|^2\sum_\ell\|\delta Q^{(\ell)}\|^2}\\ &= \lim_{N\to\infty}\Xi^{-2}\|\delta Q\|^{-2}N^{-1}\sum_\ell\sum_j a_j^2\langle\delta Q^{(\ell)},u_j\rangle^2\\ &= \Xi^{-2}\left(\sum_j a_j^2\sigma_j^2\right)\Big/\left(\sum_j a_j^2\right)\leqslant\varepsilon^2. \end{aligned}$$

Thus the vector δQ is not in the cone. Since W_1 is in the cone it follows that $\ker\pi = 0$ and therefore that the dimensions of W_1 and W are the same. □

Appendix B. Perturbations of the limit cycle and proofs about IRCs

The first step in this analysis is to calculate the linear part of the perturbation $\delta\gamma$ of the periodic orbit when a parameter is changed. This is a result of standard theory (see Hartman, 1964) and related formulas are discussed in Hwang et al. (1978).

B.1. Perturbations and IRCs: Unforced (free-running) case

We consider the differential equation

$$\dot y = g(y,k), \tag{B.1}$$

where $y = (y_1,\dots,y_n)\in R^n$ and k is a parameter. We are assuming that the equation is autonomous and hence unforced, or forced with a forcing that is constant in time. For clocks this corresponds to the case where the environmental forcing by light or temperature is unchanging in time.

We assume that Eq. (B.1) has a attracting periodic solution $y = \gamma_0(t)$ with period $\tau = \tau_0$ when $k = k_0$. We consider how this solution changes as k is varied. To do this we follow the treatment in Hartman (1964).

B.1.1. Setting up an appropriate coordinate system

We fix a point $y_0 = \gamma_0(0)$ on the periodic solution and consider a small $(n-1)$-dimensional hyperplane Σ which meets the periodic solution at the point y_0 and is transversal to the solution. For example, one could take Σ to be the plane normal to the tangent vector to the periodic solution at y_0. Near to y_0 there is a coordinate system $x = (x_1,\dots,x_n)$ such that (a) $x\in\Sigma$ if and only if $x_1 = 0$, (b) in this coordinate system, $y_0 = \underline{0} = (0,\dots,0)$ and $g(y_0,k_0) = (1,0,\dots,0)$. Let the

differential equation (B.1) in the new coordinate system be given by

$$\dot{x} = f(x,k) \tag{B.2}$$

and the periodic orbit be given by $x = \gamma_0(t)$. We consider solutions $Y(t) = Y(t,x_0,k)$ of the matrix variational equation

$$\dot{x} = f(x,k), \quad \dot{Y} = A(t)\cdot Y, \quad x(0) = x_0, \quad Y(0) = I. \tag{B.3}$$

Here $x(t) = x(t,x_0,k)$ is the solution of $\dot{x} = f(x,k)$ with initial condition x_0, $Y(t) = Y(t,x_0,k)$ is a $n \times n$ matrix and $A(t) = A(t,x,k)$ is the Jacobian matrix of partial derivatives $(\partial f_i/\partial x_j)$ evaluated at $x = x(t)$ and k and the initial condition for this solution is that $Y(0)$ is the identity matrix I. If for the matrix $Y(\tau_0)$ the eigenvalue 1 is simple then, for k near k_0, system (B.3) has a unique periodic orbit $x = \gamma_k(t)$ near $x = \gamma_0(t)$. This limit cycle varies smoothly with k. Let $\tau(k)$ be the period of γ_k and let $x_0(k)$ be the point where γ_k intersects Σ.

Firstly we ask how the period and the point x_0 change as a function of k_i. It is not too difficult to find their first derivatives which are given by the following equation:

$$\begin{bmatrix} \partial\tau/\partial k_i \\ \partial x_0/\partial k_i \end{bmatrix}_{k=k_0} = -(Y(\tau_0) - \mathrm{diag}[0, I_{n-1}])^{-1} \tag{B.4}$$

$$\times Y(\tau_0)\int_0^{\tau_0} Y(\phi)^{-1} b_i(\phi)\,\mathrm{d}\phi, \tag{B.5}$$

where $Y(t)$ stands for $Y(t,x_0(k_0),k_0)$ and $b_i(\phi)$ is $\partial f/\partial k_i$ evaluated at $x = \gamma_0(\phi)$ and $k = k_0$.

Let $\xi(t,x,k)$ denote the solution of the differential equation with initial condition $x_0 = x_0(k)$. To obtain this equation we note that the point $x_0(k)$ satisfies $\xi(t,x_0(k),k) = x_0(k)$, differentiate this equation with respect to k and solve for the left-hand side of Eq. (B.5). Then we use the results of Hartman (1964) expressing the derivatives $\partial\xi/\partial x_0$ and $\partial\xi/\partial k_i$ in terms of $Y(t)$.

The limit cycle is given by $\gamma_k(t) = \xi(t,x_0,k)$. Thus

$$\frac{\partial}{\partial k}\gamma_k(t) = \frac{\partial\xi}{\partial x_0}(t,x_0,k)\cdot\frac{\partial x_0}{\partial k} + \frac{\partial\xi}{\partial k}(t,x_0,k).$$

The term $\partial\xi(t,x_0,k)/\partial x_0$ is given by $Y(t)$ because it satisfies $\dot{Y} = A(t)Y$; $\partial x_0/\partial k$ is given by Eq. (B.5); and the last term is given by

$$Y(\tau_0)\cdot\int_0^t Y(\phi)^{-1}\cdot b_i(\phi)\,\mathrm{d}\phi = \frac{\partial\xi}{\partial k}(t,x_0,k)$$

because it satisfies the equation $\dot{Y} = A(t)Y + b_i(t)$.

From this one can show that, if the change in γ_k arising from a change δk in k is $\partial_k\gamma\cdot\delta k = \sum_i(\partial_k\gamma)_i\cdot\delta k_i$, then

$$(\partial_k\gamma)_i = -Y(t)\pi_2(Y(\tau_0) - \mathrm{diag}[0, I_{n-1}])^{-1} \times Y(\tau_0)\int_0^{\tau_0} Y(\phi)^{-1} b_i(\phi)\,\mathrm{d}\phi \tag{B.6}$$

$$+ Y(t)\int_0^t Y(\phi)^{-1} b_i(\phi)\,\mathrm{d}\phi, \tag{B.7}$$

where $\pi_2(x_1,\ldots,x_n) = (0,x_2,\ldots,x_n)$.

Thus if we only change the parameter value between ϕ_1 and ϕ_2 then the change in the limit cycle and its period is given by

$$\delta\gamma(t) = \sum_i \delta k_i\cdot\int_{\phi_1}^{\phi_2} f_{k_i,\gamma,t}(\phi)\,\mathrm{d}\phi + O(\|\delta k\|^2) \tag{B.8}$$

and

$$\delta\tau = \sum_i \delta k_i\cdot\int_{\phi_1}^{\phi_2} f_{k_i,period}(\phi)\,\mathrm{d}\phi + O(\|\delta k\|^2), \tag{B.9}$$

where

$$f_{k_i,\gamma,t}(\phi) = -Y(t)\cdot\pi_2(Y(\tau_0) - \mathrm{diag}[0, I_{n-1}])^{-1} \times Y(\tau_0)Y(\phi)^{-1} b_i(\phi)\,\mathrm{d}\phi + \tau_0^{-1} Y(t)\cdot\int_0^t Y(\sigma)^{-1} b_i(\sigma)\,\mathrm{d}\sigma$$

and

$$f_{k_i,period}(\phi) = \pi_1(Y(\tau_0) - \mathrm{diag}[0, I_{n-1}])^{-1} \times Y(\tau_0)Y(\phi)^{-1} b_i(\phi)\,\mathrm{d}\phi. \tag{B.10}$$

Definition B.1. $f_{k_i,\gamma,t}(\phi)$ and $f_{k_i,period}(\phi)$ are called *the universal IRCs for unforced systems* because all the other IRCs can be calculated from them.

We are now in a position to prove Theorem 6 for unforced systems but firstly recall the definition of the normalized limit cycle $\tilde{\gamma}$ given in Section 3.2.2. Since $\gamma_k(t) = \xi(t,x_0(k),k)$, $\tilde{\gamma}_k(t) = \xi(t\tau(k),x_0(k),k)$ and therefore

$$\theta_i(t) = \frac{\partial}{\partial k_i}\bigg|_{k=k_0}\tilde{\gamma}_k(t) = t\frac{\partial\tau}{\partial k_i}\bigg|_{k=k_0}\frac{\partial\xi}{\partial t} + \frac{\partial}{\partial k}\gamma_k(t\tau_0) = t\frac{\partial\tau}{\partial k_i}\bigg|_{k=k_0} f(\gamma_0(\tau_0 t),k_0) + \frac{\partial}{\partial k}\gamma_k(t\tau_0). \tag{B.11}$$

The last term is given by Eq. (B.7) above. Thus we see that

$$\delta\tilde{\gamma}(t) = \sum_i \delta k_i\cdot\int_{\phi_1}^{\phi_2}\tilde{f}_{k_i,\gamma,t}(\phi)\,\mathrm{d}\phi + O(\|\delta k\|^2), \tag{B.12}$$

where $\tilde{f}_{k_i,\gamma,t}(\phi) = f_{k_i,\gamma,t}(\phi) + tf(\gamma_0(\tau_0 t),k_0)f_{k_i,period}(\phi)$.

Proof of Theorem 6 (for unforced systems). The changes δQ_j caused to the output variable Q_j by variations δk_i in the parameter k_i are linear functions of the change $\delta\tau$ in the period and the change $\delta\tilde{\gamma}(t)$ of the limit cycle. Let us write this relationship $\delta Q_j = L_j\cdot(\delta\tilde{\gamma},\delta p)$. It follows

immediately from Eqs. (B.8), (B.9) and (B.12) that there is a function f_{k_i,Q_j} satisfying Eq. (9). The fact that it is unique follows because it satisfies Eq. (9) for all appropriate ϕ_1 and ϕ_2. □

B.2. Entrained forced case

The case where the system is entrained to the periodic forcing is more straightforward. Firstly, we do not have to worry about changing the coordinate system as above. Secondly, we can ignore changes in the period so long as the system stays entrained.

We consider the system

$$\dot{y} = g(t, y, k), \tag{B.13}$$

where $y = (y_1, \ldots, y_n) \in R^n$, $k = (k_1, \ldots, k_s)$ is the vector of parameters and $g(t + \tau, y, k) \equiv g(t, y, k)$. We assume that Eq. (B.13) has a attracting periodic solution $y = \gamma_0(t)$ with period $\tau = \tau_0$ when $k = k_0$. As above we consider solutions $Y(t) = Y(t, x_0, k)$ of the matrix variational equation

$$\dot{y} = g(t, y, k), \quad \dot{Y} = A(t) \cdot Y, \quad y(0) = x_0, \quad Y(0) = I. \tag{B.14}$$

Here $Y(t) = Y(t, x_0, k_0)$ is a $n \times n$ matrix and $A(t) = A(t, x, k)$ is the Jacobian matrix of partial derivatives $(\partial f_i/\partial x_j)$ evaluated at $t, x = x(t)$ and $k = k_0$. The initial condition for this solution is that $Y(0)$ is the identity matrix I. If the matrix $Y(\tau_0)$ does not have 1 as an eigenvalue then, for k near k_0, the system (B.14) has a unique periodic orbit $y = \gamma_k(t)$ near $y = \gamma_0(t)$. Moreover, these periodic orbits satisfy

$$\frac{\partial}{\partial k_i}\gamma_k(t)\bigg|_{k=k_0} = -(Y(\tau_0) - I)^{-1} \cdot Y(\tau_0) \times \int_0^p Y(s)^{-1} \cdot b_i(s)\,\mathrm{d}s. \tag{B.15}$$

Here the vector $b_i(s)$ is $\partial f/\partial k_i$ evaluated at $y = \gamma_0(t)$ and $k = k_0$. This is proved in a similar fashion to the proof for Eq. (B.7) above.

For the universal IRC in this case we only have to consider $f_{k_i,\gamma,t}(\phi)$ since period variations are not relevant. In this case, if the change in the parameters is only applied between ϕ_1 and ϕ_2, the change in the limit cycle (as in Eq. (B.8)) is given by

$$\delta\gamma(t) = \sum_i \delta k_i \cdot \int_{\phi_1}^{\phi_2} f_{k_i,\gamma,t}(\phi)\,\mathrm{d}\phi + O(\|\delta k\|^2), \tag{B.16}$$

where

$$f_{k_i,\gamma,t}(\phi) = -Y(t)\bigg(\pi_2(Y(\tau_0) - I)^{-1} Y(\tau_0) Y(\phi)^{-1} b_i(\phi) + \tau_0^{-1} \int_0^t Y(\sigma)^{-1} b_i(\sigma)\,\mathrm{d}\sigma\bigg). \tag{B.17}$$

Proof of Theorem 6 (for forced systems). The proof proceeds in a similar fashion to the unforced case. □

B.3. Calculation of the circle perturbations

We now consider the normalised limit cycle $\tilde{\gamma}_k$. The partial derivatives of this are given by Eq. (B.11) where, for the forced and entrained case, the first term is zero.

To approximate the linear operator $M^* : \delta k \to (\delta\tilde{\gamma}, \delta\tau)$ one can proceed as follows. In terms of the quantities $\theta_i(t) = \partial\tilde{\gamma}_k(t)/\partial k_i|_{k=k_0}$ which are calculated above in Eq. (B.11), the operator M^* is given by

$$M^* \cdot \delta k = \sum_i \delta k_i \cdot \theta_i.$$

Thus if $\bar{\theta}_i$ is the vector given by $(\bar{\theta}_i)_j = \theta_i(j/N)$, (where N is a large integer), an approximation $M^{(N)}$ of M^* is given by

$$M^{(N)} \cdot \delta k = \sum_i \delta k_i \cdot \bar{\theta}_i.$$

This gives a matrix representation for $M^{(N)}$ in terms of the basis vectors $\bar{\theta}_i$. This approach corresponds to approximating $\delta\tilde{\gamma} = \delta\tilde{\gamma}(t)$ by the vector $\overline{\delta\gamma}$ whose jth entry is $\delta\tilde{\gamma}(j/N)$.

We have developed a software tool that rapidly calculates the quantities $\theta_i(t)$. Using the above results this enables us to compute M^* and its singular value decomposition to arbitrary accuracy. An example of such a calculation is given in Fig. 3.

B.4. Perturbations and Floquet multipliers

Let $\rho_1, \ldots, \rho_k$ be the eigenvalues of $Y(\tau_0)$ and suppose that ρ_ℓ has multiplicity n_ℓ so that $n_1 + n_2 + \cdots + n_k = n$. For each ℓ there are vectors $z_1^{(\ell)} = z_1^{(\ell)}(t), \ldots, z_{n_\ell}^{(\ell)} = z_{n_\ell}^{(\ell)}(t)$, which are periodic in t with period τ_0, such that each of the following are independent solutions of

$$\dot{Y} = A(t) \cdot Y \tag{B.18}$$

in Eq. (B.3) or (B.14)

$$\left(z_1^{(\ell)}\frac{t^m}{m!} + z_2^{(\ell)}\frac{t^{m-1}}{(m-1)!} + \cdots + z_m^{(\ell)}t + z_{m+1}^{(\ell)}\right)\rho_\ell^{-t/\tau_0}, \quad (m = 0, 1, \ldots, n_\ell - 1).$$

Every solution of Eq. (B.18) is a linear combination of these. For clarity consider the generic case where the eigenvalues are all simple (i.e. $n_\ell \equiv 1$). Suppose that $\rho_1, \ldots, \rho_r$ are real and $\rho_{r+1}, \ldots, \rho_n$ are complex and $\rho_j = \mathrm{e}^{\tau_0\chi_j}$. Then there are vectors $z_j(t)$, $j = 1, \ldots, r$ and pairs of vectors $z_j(t) = (z_j^{(a)}(t), z_j^{(b)}(t))$, $j = r+1, \ldots, n$; each periodic in t with period τ_0 such that every solution of Eq. (B.18) is a linear combination of the functions $z_j(t)\mathrm{e}^{t\chi_j}$ ($j = 1, \ldots, r$ where χ_j is real) and $z_j^{(a)}(t)\mathrm{e}^{a_j t}\cos\theta_j t$ and $z_j^{(b)}(t)\mathrm{e}^{a_j t}\sin\theta_j t$ ($j = r+1, \ldots, n$ where $\chi_j = a_j + i\theta_j$

is complex). This means that the matrices $Y(t)$ map the vectors $z_j(0)$ to $z_j(t)$ for $j=1,\ldots,r$ and, if $V_j(t)$ is the two-dimensional space spanned by $z_j^{(a)}(t)$ and $z_j^{(b)}(t)$ for $j=r+1,\ldots,n$, then $Y(t)$ maps $V_j(0)$ onto $V_j(t)$ and acts as a rotation through $\theta_j t$ with respect to the given basis. It follows from this that

$$\frac{\partial}{\partial k_i}\gamma_k(t)\bigg|_{k=k_0} = \sum_m (\rho_m-1)^{-1} z_m(t) \times \int_t^{t+\tau_0} \mathrm{e}^{\chi_m(t+\tau_0-\phi)} b_{i,m}(\phi)\,\mathrm{d}\phi, \qquad \text{(B.19)}$$

where $b_i(t)=\sum_m b_{i,m}(t)z_m(t)$ and if ρ_m is real the summand has the obvious meaning while if it is complex then the summand should be interpreted appropriately: $z_m(t)$ is the complex vector $z_j^{(a)}(t)+iz_j^{(b)}(t), b_{i,m}(t)=b_{i,m}^{(a)}(t)+ib_{i,m}^{(b)}(t)$ where $b_{i,m}(t)$ is the projection of $b_i(t)$ into $V_m(t)$ and the summand is the usual vector in $V_m(t)$ obtained by taking real and imaginary parts. Each χ_m is negative and if it is not too close to zero then we can approximate the integral in Eq. (B.19) by $\chi_m^{-1}b_{i,m}(t)$. The error terms are $O(\chi_m^{-2})$ or $O(e^{-\tau_0\chi_m})$. Thus we can write

$$\frac{\partial}{\partial k_i}\gamma_k(t)\bigg|_{k=k_0} \approx \sum_{m:\chi_m\sim 0} (\rho_m-1)^{-1} z_m(t) \times \int_t^{t+\tau_0} \mathrm{e}^{\chi_k(t+\tau_0-\phi)} b_{i,m}(\phi)\,\mathrm{d}\phi + \sum_{k:\chi_m\sim 0} \frac{b_{i,k}(t)}{(\rho_m-1)\chi_m} z_m(t). \qquad \text{(B.20)}$$

From this we see that in the direction of the eigenspace corresponding to χ_m, the magnitude of the perturbation is $O(1/|\chi_m|)$.

B.5. Proof that IRC for period gives a PRC

In this we use the notation of Section B.1.1. Thus we consider system (B.2) given by $\dot{x}=f(x,k)$. The point y_0, the cross section Σ and the coordinate system $x=(x_1,\ldots,x_n)$ are as in Section B.1.1. We let π_1 denote the projection $\pi_1(x)=x_1$. Since the vector field at y_0 is $(1,0,\ldots,0)$, it follows that if $x(t)=\gamma_0(t)$ is the periodic orbit ($x(0)=y_0$) then $\pi_1(x(t))=t+O(t^2)$.

Lemma B.2. *Suppose that $\xi(t,x,k)$ is the flow of the dynamical system* (B.2) *so that $\xi(t,y_0,k_0)$ is the periodic orbit. Then the phase of $\xi(\tau_0,y_0(k),k)$ equals $\sigma=\pi_1(\xi(\tau(k),y_0(k),k))$ up to an error which is $O(\sigma^2)$ and*

$$\frac{\partial\sigma}{\partial k_i}=-\frac{\partial\tau}{\partial k_i}.$$

Proof. Since $\xi(\tau(k),y_0(k),k)=y_0(k)$ we have

$$\frac{\partial\xi}{\partial y_0}\cdot\frac{\partial y_0}{\partial k_i}+\frac{\partial\xi}{\partial k_i}=\frac{\partial y_0}{\partial k_i}-\frac{\partial\xi}{\partial t}\cdot\frac{\partial\tau}{\partial k_i},$$

where the partial derivatives of ξ are calculated at $(t,y,k)=(\tau_0,y_0(k_0),k_0)$ and the other partial derivatives are calculated at $k=k_0$. Thus

$$\frac{\partial\sigma}{\partial k_i}=\frac{\partial}{\partial k_i}\pi_1(\xi(\tau_0,y_0(k),k))=\pi_1\left(\frac{\partial\xi}{\partial y_0}\cdot\frac{\partial y_0}{\partial k_i}+\frac{\partial\xi}{\partial k_i}\right) =\pi_1\left(\frac{\partial y_0}{\partial k_i}-\frac{\partial\xi}{\partial t}\cdot\frac{\partial\tau}{\partial k_i}\right)=-\frac{\partial\tau}{\partial k_i}$$

since $\pi_1(\partial y_0/\partial k_i)=0$ and $\partial\xi/\partial t=(1,0,\ldots,0)$ so that $\pi_1(\partial\xi/\partial t)=1$ and $\pi_1((\partial\xi/\partial t)\cdot(\partial\tau/\partial k_i))=(\partial\tau/\partial k_i)\cdot\pi_1(\partial\xi/\partial t)$. □

Appendix C. Numerical calculation of IRCs and intelligent orienteering in parameter space

The calculation of the IRCs was performed in Matlab and we will make available via our website www.maths.ac.uk/ipcr/ a Matlab software tool that we have written that allows one to analyse clock models given by differential equations. In particular this tool can calculate the IRCs f_{k_i,Q_j}, the operator M^* and the principal components of Sections 3.4.2 and B.3. It can also be used to make user-specified changes to the outputs by varying parameters, and to integrate the equations and compare the forced and unforced behaviours.

The calculation of IRCs is straightforward using Eq. (B.8) or Eqs. (B.17) and (B.10) except for one issue. In order to obtain IRCs given by Eq. (B.8) or Eqs. (B.17) and (B.10) we need to calculate the matrix $Y(t)^{-1}$ and unfortunately, since $\|Y(t)^{-1}\|\sim\exp At$, where A is typically quite large, the computation blows up rather quickly as t is increased towards τ_0. This issue is addressed in Hwang et al. (1978) and we used similar ideas to overcome the blowup.

The results of this paper can also be used to perform intelligent orienteering or tuning in parameter space to achieve certain user-required changes in the phenotype of the clock model and we have incorporated such an approach into the software tool mentioned above.

References

Albrecht, U., Zheng, B., Larkin, D., Sun, Z.S., Lee, C.C., 2001. Mper1 and mper2 are essential for normal resetting of the circadian clock. J. Biol. Rhythms 16 (2), 100–104.

Cheng, P., Yang, Y.H., Liu, Y., 2001. Interlocked feedback loops contribute to the robustness of the neurospora circadian clock. Proc. Natl Acad. Sci. USA 98 (13), 7408–7413.

Cyran, S.A., Buchsbaum, A.M., Reddy, K.L., Lin, M.C., Glossop, N.R., Hardin, P.E., Young, M.W., Storti, R.V., Blau, J., 2003. vrille, pdp1, and dclock form a second feedback loop in the drosophila circadian clock. Cell 112 (3), 329–341.

Daan, S., Albrecht, U., van der Horst, G.T.J., Illnerova, H., Roenneberg, T., Wehr, T.A., Schwartz, W.J., 2001. Assembling a clock for all seasons: are there m and e oscillators in the genes? J. Biol. Rhythms 16 (2), 105–116.

Eriksson, M.E., Hanano, S., Southern, M.M., Hall, A., Millar, A.J., 2003. Response regulator homologues have complementary, light-dependent functions in the arabidopsis circadian clock. Planta 218 (1), 159–162.

Forger, D.B., Peskin, C.S., 2003. A detailed predictive model of the mammalian circadian clock. Proc. Natl Acad. Sci. USA 100 (25), 14806–14811.

Garceau, N.Y., Liu, Y., Loros, J.J., Dunlap, J.C., 1997. Alternative initiation of translation and time-specific phosphorylation yield multiple forms of the essential clock protein frequency. Cell 89 (3), 469–476.

Glossop, N.R.J., Lyons, L.C., Hardin, P.E., 1999. Interlocked feedback loops within the drosophila circadian oscillator. Science 286 (5440), 766–768.

Goldbeter, A., 2002a. Computational approaches to cellular rhythms. Nature 420 (6912), 238–245.

Goldbeter, A., 2002b. Computational biology of circadian rhythms. Mol. Biol. Cell 13, 57.

Gonze, D., Roussel, M.R., Goldbeter, A., 2002. A model for the enhancement of fitness in cyanobacteria based on resonance of a circadian oscillator with the external light- dark cycle. J. Theor. Biol. 214 (4), 577–597.

Guckenheimer, J., Holmes, P., 1983. Nonlinear oscillations, dynamical systems and bifurcations of vector fields. Applied Mathematical Sciences. Springer, New York.

Harmer, S.L., Hogenesch, L.B., Straume, M., Chang, H.S., Han, B., Zhu, T., Wang, X., Kreps, J.A., Kay, S.A., 2000. Orchestrated transcription of key pathways in arabidopsis by the circadian clock. Science 290 (5499), 2110–2113.

Hartman, P., 1964. Ordinary Differential Equations. Wiley, New York.

Hwang, J.T., Dougherty, E.P., Rabitz, S., Rabitz, H., 1978. The green's function method of sensitivity analysis in chemical kinetics. J. Chem. Phys. 69 (11), 5180–5191.

Johnson, C.H., Elliott, J.A., Foster, R., 2003. Entrainment of circadian programs. Chronobiol. Int. 20 (5), 741–774.

Lee, K., Loros, J.J., Dunlap, J.C., 2000. Interconnected feedback loops in the neurospora circadian system. Science 289 (5476), 107–110.

Leloup, J.C., Goldbeter, A., 2003. Toward a detailed computational model for the mammalian circadian clock. Proc. Natl Acad. Sci. USA 100 (12), 7051–7056.

Leloup, J.C., Gonze, D., Goldbeter, A., 1999. Limit cycle models for circadian rhythms based on transcriptional regulation in drosophila and neurospora. J. Biol. Rhythms 14 (6), 433–448.

Oster, H., Yasui, A., van der Horst, G.T., Albrecht, U., 2002. Disruption of mcry2 restores circadian rhythmicity in mper2 mutant mice. Genes Dev. 16 (20), 2633–2638.

Ostlund, S., Rand, D., Sethna, J., Siggia, E., 1983. Universal properties of the transition from quasi-periodicity to chaos in dissipative systems. Physica D 8 (3), 303–342.

Preitner, N., Damiola, F., Lopez-Molina, L., Zakany, J., Duboule, D., Albrecht, U., Schibler, U., 2002. The orphan nuclear receptor rev-erbalpha controls circadian transcription within the positive limb of the mammalian circadian oscillator. Cell 110 (2), 251–260.

Press, W.H., Flanner, B.P., Teukolsky, S.A., Vetterling, W., 1988. Numerical Recipes in C. Cambridge University Press, Cambridge.

Reddy, A.B., Field, M.D., Maywood, E.S., Hastings, M.H., 2002. Differential resynchronisation of circadian clock gene expression within the suprachiasmatic nuclei of mice subjected to experimental jet lag. J. Neurosci. 22 (17), 7326–7330.

Rensing, L., Ruoff, P., 2002. Temperature effect on entrainment, phase shifting, and amplitude of circadian clocks and its molecular bases. Chronobiol. Int. 19 (5), 807–864.

Roenneberg, T., Merrow, M., 2003. The network of time: understanding the molecular circadian system. Curr. Biol. 13 (5), R198–207.

Ruoff, P., 2000. Temperature compensation in biological oscillators: a challenge for joint experimental and theoretical analysis. Comments Theor. Biol. 5 (6), 361–382.

Smolen, P., Baxter, D.A., Byrne, J.H., 2001. Modeling circadian oscillations with interlocking positive and negative feedback loops. J. Neurosci. 21 (17), 6644–6656.

Tyson, J.J., Hong, C.I., Thron, C.D., Novak, B., 1999. A simple model of circadian rhythms based on dimerization and proteolysis of per and tim. Biophys. J. 77 (5), 2411–2417.

Ueda, H.R., Hagiwara, M., Kitano, H., 2001. Robust oscillations within the interlocked feedback model of drosophila circadian rhythm. J. Theor. Biol. 210 (4), 401–406.

Winfree, A., 2001. The Geometry of Biological Time. Springer, New York.

Young, M.W., Kay, S.A., 2001. Time zones: a comparative genetics of circadian clocks. Nature Rev. Genet. 2 (9), 702–715.

Zheng, B., Albrecht, U., Kaasik, K., Sage, M., Lu, W., Vaishnav, S., Li, Q., Sun, Z.S., Eichele, G., Bradley, A., Lee, C.C., 2001. Nonredundant roles of the mper1 and mper2 genes in the mammalian circadian clock. Cell 105 (5), 683–694.